

UCSF

UC San Francisco Electronic Theses and Dissertations

Title

Neonatal gut-microbiome-derived 12,13 DiHOME impedes tolerance and promotes childhood atopy and asthma

Permalink

<https://escholarship.org/uc/item/1dm589kh>

Author

Levan, Sophia Rose

Publication Date

2018

Peer reviewed|Thesis/dissertation

Neonatal gut-microbiome-derived 12,13 DiHOME impedes tolerance
and promotes childhood atopy and asthma

by

Sophia Rose Levan

DISSERTATION

Submitted in partial satisfaction of the requirements for the degree of

DOCTOR OF PHILOSOPHY

in

Biomedical Sciences

in the

GRADUATE DIVISION

Copyright 2018

by

Sophia Levan

ACKNOWLEDGEMENTS

I would like to thank my mentor Dr. Susan Lynch, the members of the Lynch lab, my family, and friends for supporting me through this process. Let's hope this is the first of many great adventures.

CONTRIBUTIONS TO THE PRESENTED WORK

The work described in this dissertation was done under the direct supervision of Dr. Susan V. Lynch PhD. Additional guidance was provided by members of the thesis committee: Dr. Anita Sil MD/PhD and Dr. Clifford A. Lowell MD/PhD.

Contents in Chapter 2 and 3 are modified from the following unpublished manuscript:

Levan, S. R., Stamnes, K. A., Lin, D. L., Fujimura, K. E., Ownby, D. R., Zoratti, E. M., Boushey, H. A., Johnson, C. C., Lynch, S. V. *Unpublished*, May 2018. *Neonatal gut-microbiome-derived 12,13 DiHOME impedes tolerance and promotes childhood atopy and asthma*. SRL designed the study, performed research, developed the manuscript; KAS, performed research and contributed to manuscript development; DLL and KEF, performed research; DRO, EMZ and CCJ provided samples and data from the WHEALS cohort and contributed to manuscript development; HAB contributed to manuscript development; SVL, designed the study, developed the manuscript. All authors reviewed and approved this manuscript.

Neonatal gut-microbiome-derived 12,13 DiHOME impedes tolerance and promotes childhood atopy and asthma

Sophia Rose Levan

ABSTRACT

Neonates at risk of childhood atopy and asthma are characterized by gut microbiome perturbation and fecal enrichment of 12,13 DiHOME. However, the underlying mechanism and source of this metabolite in neonates remain poorly understood. Here we show that 12,13 DiHOME treatment of human dendritic cells altered peroxisome proliferator-activated receptor γ regulated gene expression and decreased immune tolerance. In mice, 12,13 DiHOME treatment prior to airway challenge exacerbated pulmonary inflammation and decreased lung regulatory T cells. Metagenomic sequencing identified approximately 1,400 bacterial epoxide hydrolase genes in neonatal feces. Three of which could produce 12,13 DiHOME *in vitro*. In our neonatal cohort, these three strain-specific bacterial genes and their product, 12,13 DiHOME, are associated with increased odds of atopy and asthma development in childhood, suggesting that early-life gut-microbiome risk factors may shape immune tolerance and identify high-risk neonates years in advance of clinical symptoms.

TABLE OF CONTENTS

CHAPTER 1: INTRODUCTION	1
CHAPTER 2: Neonatal gut-microbiome-derived 12,13 DiHOME impedes tolerance and promotes childhood atopy and asthma	5
Abstract	6
Main Text	6
12,13 DiHOME acts via PPAR γ on DCs to decrease Tregs	6
12,13 DiHOME exacerbates lung inflammation in allergen-challenged mice	9
12,13 DiHOME is significantly enriched in the feces of neonates at risk of atopy and asthma	11
Specific Strains of <i>Bifidobacterium</i> and <i>Enterococcus</i> can produce 12,13 DiHOME	14
Strain-specific bacterial EH genes and their product, 12,13 DiHOME, are associated with the development of atopy and asthma in childhood	15
Material and Methods	17
Human Immune Assays	17
Luciferase Assay	18
Animal Models.....	19
Study Population and Definitions	21
Neonatal Subset Characteristics	22
Mass Spectrometry in Human Samples	23
Metagenomic Data Analysis.....	23
Colorimetric Detection of EH Activity	24

Quantification of 3EH Copy Number by qPCR.....	26
Statistical Analysis	26
Data and materials availability	27
Supplementary Figures and Tables	28
Acknowledgements	46
CHAPTER 3: Implications and Future Directions	47
REFERENCES	50

LIST OF TABLES

Tables

TABLE 1: Comparison of sample characteristics for atopy at age two and asthma at age four. 16

Supplemental Tables

SUPPLEMENTAL TABLE 1: Conserved marker regions for the top differential EH genes found in the metagenomic sequencing data. 37

SUPPLEMENTAL TABLE 2: Antibodies used for human and mouse immune cell staining. 38

SUPPLEMENTAL TABLE 3: Primers used for human, mouse, and bacterial qPCR. 39

SUPPLEMENTAL TABLE 4: Sequences of the synthetic EH gene constructs used in *the in vitro* screen on EH activity 40

SUPPLEMENTAL TABLE 5: Gene fragments used to generate the standard curves for quantification of the 3EH genes by qPCR 44

SUPPLEMENTAL TABLE 6: Estimated odds ratio based on univariate logistical regression models of atopy at age two or asthma at age four 45

LIST OF FIGURES

Figures

- FIGURE 1:** 12,13 DiHOME acts via PPAR γ on DCs to decrease Tregs 8
- FIGURE 2:** Peritoneal treatment with 12,13 DiHOME exacerbates lung inflammation in CRA-challenged mice. 11
- FIGURE 3:** *Enterococcus faecalis* and *Bifidobacterium bifidum* strains in the neonatal gut microbiome encode the capacity to produce 12,13 DiHOME and increase the odds of developing atopy at age two or asthma at age four. 13

Supplemental Figures

- SUPPLEMENTAL FIGURE 1:** 12,13 DiHOME treatment of DCs decreases IL-10 secretion and Treg frequency without affecting cell viability. 30
- SUPPLEMENTAL FIGURE 2:** Peritoneal treatment with 12,13 DiHOME exacerbates innate immune infiltration in the lungs of CRA-challenged mice. 32
- SUPPLEMENTAL FIGURE 3:** Bacterial EH enzymes can generate 9,10 and 12,13 DiHOME . 33
- SUPPLEMENTAL FIGURE 4:** The distributions of 12,13 DiHOME concentration and 3EH copy number were skewed in our subset of the WHEALS cohort (n=41). 34
- SUPPLEMENTAL FIGURE 5:** Alignment of thirteen EH candidate genes 36

CHAPTER 1: INTRODUCTION

Asthma is the most common chronic childhood disease worldwide (Sminkey). Childhood allergic asthma refers to the development of severe asthma before age twelve. Children with this disease often have a history of allergic sensitization to multiple food and aeroallergens and a family history of allergic disease (Havstad et al., 2014; Simpson et al., 2010). Immunologically, these children are characterized by a significant decrease of regulatory T cells (Tregs) in their bronchoalveolar lavage fluid (Hartl et al., 2007). While genetic risk factors have been associated with childhood allergic asthma, the prevalence of the disease in developed countries is increasing at a rate that cannot be explained by genetics alone, suggesting that our changing environment may play a role in its development (Fujimura and Lynch, 2015; Ober and Yao, 2011).

The hypothesis that early-life environment may play a role in the development of childhood allergic asthma is supported by several recent studies that have shown associations between early-life environmental exposures and the subsequent development of disease. These include the observations that formula feeding, birth by Caesarian section, and pre- and postnatal antibiotic use are associated with increased risk of disease, while early-life exposure to livestock and furred pets are protective (Chu et al., 2017; Fall et al., 2015; Genuneit, 2012; Gerlich et al., 2017; Mitre et al., 2018; Silvers et al., 2012; Yamamoto-Hanada et al., 2017). All of these early-life environmental exposures are also known to shape the composition and function of the early-life microbiome (Arrieta et al., 2014; Dominguez-Bello et al., 2010; Fujimura et al., 2014a; Gonzalez-Perez et al., 2016; Langdon et al., 2016).

The human microbiome refers to the community of bacteria, viruses, and fungi that live in and on our bodies. Recent advances in DNA sequencing have revealed diverse and dynamic communities of organisms that persist on our skin, gut, and mucus membranes (Donaldson et al., 2016; Knight et al., 2017). In adults, these microbial communities and their metabolic products are associated with both health and disease (Gilbert et al., 2016; Lynch and Pedersen, 2016). In very early-life these microbial communities are simpler and less diverse but rapidly

increase in complexity with increasing chronological age (Bäckhed et al., 2015; Durack et al., 2018).

Recently several studies, by our group and others, investigated the role of the early-life microbiome in the development of childhood allergic asthma. We found that neonates (~1 month old) at heightened risk of childhood allergic asthma possess a distinct microbiome that is characterized by depletion of taxonomic members of specific bacterial genera (*Akkermansia*, *Bifidobacterium*, *Faecalibacterium*) and fungal expansion (*Candida*, *Rhodotorula*) (Fujimura et al., 2016). These results recapitulate many of the observations made in a cohort of Canadian neonates, which showed similar shifts in neonatal bacterial communities associated with increased incidence of childhood disease (Arrieta et al., 2015). Additionally, untargeted mass spectrometry on neonatal stool revealed that high-risk neonatal microbiomes were associated with changes in lipid metabolism. In mice, gut-microbiome-derived short chain fatty acids protect against allergic airway inflammation (Fonseca et al., 2017; Trompette et al., 2014). Consistent with this observation, two independent birth cohorts demonstrated a depletion of polyunsaturated fatty acids in the feces of neonates at high-risk of atopy and asthma (Durack et al., 2018; Fujimura et al., 2016). Conversely, monohydroxy fatty acids and in particular, 12,13 DiHOME was significantly enriched in the feces of high-risk neonates (Fujimura et al., 2016).

To probe the potential effects of these microbial and metabolic shifts on immune cells, our lab extracted and filter-sterilized the products of the gut microbiome from the stool of high- and low-risk neonates. This milieu, which includes metabolites, was used to treat dendritic cells (DCs), isolated from healthy human donors. Human DCs were treated for two days, then washed, and subsequently co-cultured with autologous T cells. This assay revealed that the products found in the stool of high-risk neonates could increase the frequency of Th2 cells and the secretion of IL-4, while decreasing the frequency of Tregs (Fujimura et al., 2016). To identify specific metabolites that differed between high- and low-risk neonates, we performed a multivariate analysis of the metabolomics data from our cohort and found that high-risk

neonates had increased fecal concentrations of 12,13 DiHOME compared to the low-risk groups (Fujimura et al., 2016). Treatment of human DCs with this metabolite caused a dose-dependent decrease in Tregs, recapitulating the decrease observed following exposure to filter-sterilized stool from neonates at high-risk of atopy and asthma (Fujimura et al., 2016).

12,13 DiHOME is a relatively uncharacterized linoleic acid metabolite that was previously identified as a potential biomarker of established allergic asthma in adults, an inhibitor of the neutrophil respiratory burst in culture, and a regulator of lipid metabolism in human adipose and skeletal muscle (Lundström et al., 2012; Lynes et al., 2017; Stanford et al., 2018; Thompson and Hammock, 2007). The conversion of linoleic acid to 12,13 DiHOME is a two-step process. First, linoleic acid is converted to 12,13 EpOME either by a cytochrome P450 epoxygenase or by free radical oxidation (Karonen et al., 2012; Mosblech et al., 2009). Then 12,13 EpOME is converted to 12,13 DiHOME by an epoxide hydrolase (EH). Fungi, bacteria, and human cells possess the EH genes required to convert 12,13 EpOME to 12,13 DiHOME (Bahl et al., 2010; Fischer and Keller, 2016; Gomez et al., 2006; Smit, 2004), leading us to hypothesize that the neonatal gut microbiome could be a potential source of this oxylipin.

Structurally, 12,13 DiHOME resembles known ligands of peroxisome proliferator-activated receptor γ (PPAR γ), a lipid-activated nuclear receptor that regulates adipogenesis, fatty acid uptake, inflammation, and intestinal microbiota (Byndloss et al., 2017; Khare et al., 2015; Vangaveti et al., 2014; Wahli and Michalik, 2012). In mice, loss of PPAR γ in DCs leads to a loss of immune tolerance and exacerbation of pulmonary inflammation (Khare et al., 2015). However, despite its immunoregulatory effect and links to atopy and asthma in humans, the mechanism and source of 12,13 DiHOME in neonates at high-risk of atopy and asthma remain unknown.

CHAPTER 2: Neonatal gut-microbiome-derived 12,13 DiHOME impedes tolerance and promotes childhood atopy and asthma

Content in this chapter was modified from the following unpublished manuscript:

Levan, S. R., Stamnes, K. A., Lin, D. L., Fujimura, K. E., Ownby, D. R., Zoratti, E. M., Boushey, H. A., Johnson, C. C., Lynch, S. V.. *Unpublished*, May 2018. *Neonatal gut-microbiome-derived 12,13 DiHOME impedes tolerance and promotes childhood atopy and asthma.*

Abstract

Neonates at risk of childhood atopy and asthma are characterized by gut microbiome perturbation and fecal enrichment of 12,13 DiHOME. However, the underlying mechanism and source of this metabolite in neonates remain poorly understood. Here we show that 12,13 DiHOME treatment of human dendritic cells altered peroxisome proliferator-activated receptor γ regulated gene expression and decreased immune tolerance. In mice, 12,13 DiHOME treatment prior to airway challenge exacerbated pulmonary inflammation and decreased lung regulatory T cells. Metagenomic sequencing identified approximately 1,400 bacterial epoxide hydrolase genes in neonatal feces. Three of which could produce 12,13 DiHOME in vitro. In our neonatal cohort, these three strain-specific bacterial genes and their product, 12,13 DiHOME, are associated with increased odds of atopy and asthma development in childhood, suggesting that early-life gut-microbiome risk factors may shape immune tolerance and identify high-risk neonates years in advance of clinical symptoms.

Main Text

12,13 DiHOME acts via PPAR γ on DCs to decrease Tregs

Given the structural similarities between 12,13 DiHOME and known ligands of PPAR γ , we hypothesized that 12,13 DiHOME induces pro-allergic immune dysfunction via PPAR γ signaling in DCs. Accordingly, we treated human DCs with 12,13 DiHOME or vehicle and examined its effects. 12,13 DiHOME treatment decreased DC secretion of IL-10, an anti-inflammatory cytokine that protects against allergic inflammation (Figure 1a, Supplementary Figure 1a) (Iyer and Cheng, 2012). Additionally, co-culture of 12,13 DiHOME-treated DCs with autologous T cells altered the distribution of CD4⁺ T cells, specifically by decreasing the frequency of Tregs without decreasing cell viability (Figure 1b-c, Supplementary Figure 1b-c).

To evaluate whether 12,13 DiHOME exerts this effect via PPAR γ , we isolated RNA from human DCs treated with 12,13 DiHOME and examined the expression of PPAR γ -regulated

genes. 12,13 DiHOME treatment mimicked previously characterized effects of PPAR γ activation: decreased expression of CD1a, an immune marker involved in lipid presentation (Szatmari et al., 2007a); increased expression of CD36, a fatty-acid transporter implicated in 12,13 DiHOME-regulation of brown adipocytes (Lynes et al., 2017); and increased expression of FABP4 and HADH, genes involved in fatty acid uptake and metabolism (Szatmari et al., 2007a) (Figure 1d-e). To confirm these observations, we used flow cytometry to examine the effects of 12,13 DiHOME on the expression of PPAR γ -regulated proteins in human DCs. Again, 12,13 DiHOME treatment mimicked PPAR γ activation, increasing expression of CD36, and decreasing expression of CD1a, CD80, and CCR7, immune markers involved in lipid presentation, antigen presentation, and cell trafficking (Szatmari et al., 2007a), in human DCs (Figure 1f-i, Supplementary Figure 1f-g).

To test whether 12,13 DiHOME directly acts on PPAR γ , we utilized a modified PPAR γ reporter assay (Choo et al., 2015) and demonstrated that treatment with concentrations of 12,13 DiHOME in excess of 50 μ M leads to PPAR γ activation (Figure 1j). This is consistent with the increase in lipid uptake and CD36 expression observed when adipose is treated with 12,13 DiHOME (Lynes et al., 2017). While PPAR γ activation in DCs is traditionally considered anti-inflammatory (Hammad et al., 2004; Woerly et al., 2003), recent studies suggest that PPAR γ may in fact promote allergic inflammation (Nobs et al., 2017). Alternatively, 12,13 DiHOME may act as a weak agonist of PPAR γ and compete with endogenous PPAR γ ligands found in serum (Szatmari et al., 2007b).

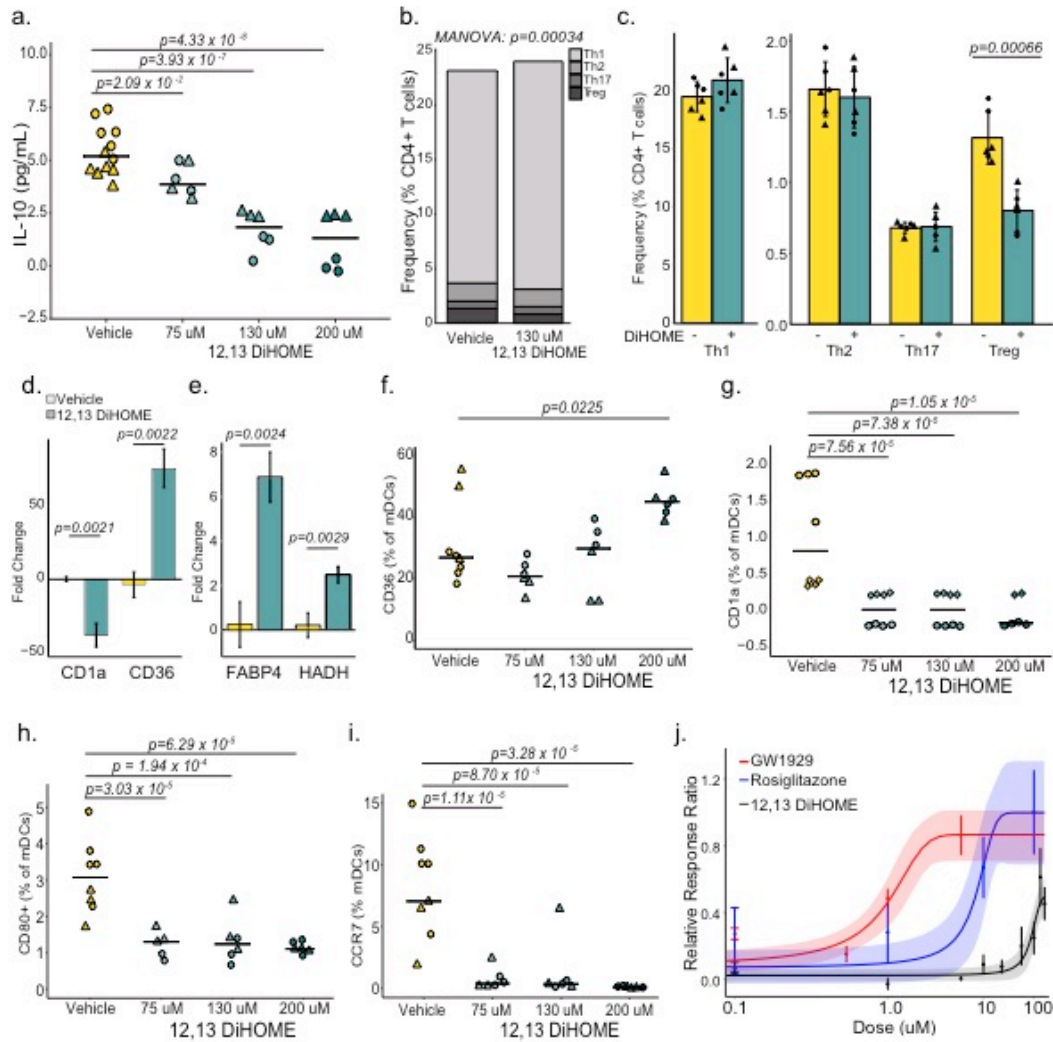


Figure 1: 12,13 DiHOME acts via PPAR γ on DCs to decrease Tregs (A) 12,13 DiHOME treatment causes a dose-dependent decrease in IL-10 secretion from human DCs [Linear Mixed Effects (LME); $p=0.0209$, $p=3.93 \times 10^{-7}$, $p=4.33 \times 10^{-8}$ for concentrations of 75, 130, 200 μM , respectively). (B,C) Treatment of DCs with 130 μM 12,13 DiHOME induces a significant shift in the distribution of helper T cells (MANOVA; $p=0.00034$) and causes a specific decrease in the frequency of Tregs (CD3+CD4+CD25+FoxP3+; LME; $p=0.00025$). (D,E) Treatment of human DCs with 130 μM 12,13 DiHOME causes changes in gene expression consistent with activation of PPAR γ (LME; $p=0.0021$, $p=0.0022$, $p=0.0024$, $p=0.0029$ for CD1a, CD36, FABP4, and HADH, respectively). (F,G,H,I) 12,13 DiHOME increases the expression of CD36 at high concentrations (LME; $p=0.0225$ for 200 μM) and decreases the expression of CD1a, CD80, and CCR7 on DCs (CD3-CD19-CD11c+; LME; $p<0.001$ for all comparisons). Figures 1a-h were performed with $n=3-4$ treatment replicates using cells isolated from 2 independent donors (biological replicates; \blacktriangle , \blacklozenge , \bullet). (J) Raw264.7 cells were transfected with a PPAR γ -activated luciferase reporter and treated with 12,13 DiHOME or known PPAR γ agonists GW1929 (Kd = 1.4 nM) (33) and Rosiglitazone (Kd = 40 nM) (34) ($n=3$). All error bars represent the standard error of the mean (SEM).

12,13 DiHOME exacerbates lung inflammation in allergen-challenged mice

We next examined whether 12,13 DiHOME exacerbates allergic sensitization *in vivo*, by treating mice with 12,13 DiHOME (30 mg/kg) or vehicle (10% DMSO) via peritoneal injection prior to airway sensitization and challenge with cockroach antigen (CRA) (Fujimura et al., 2014). Treated animals exhibit increased peribronchial and perivascular inflammatory infiltrates and serum IgE compared to those treated with vehicle alone (Figure 2a-d, Supplementary Figure 2a-b). 12,13 DiHOME-treated animals also exhibited increases in lung resident T cells, neutrophils, and monocytes, and pulmonary expression of pro-inflammatory innate cytokines, IL1 β , IL1 α , and TNF, as well as a significant decrease in the frequency of lung Tregs and a trend towards decreased lung resident alveolar macrophages (Figure 2e-g, Supplementary Figure 2g-k). These inflammatory immunologic changes may be explained by the effect of 12,13 DiHOME on PPAR γ observed *ex vivo*. Alternatively, 12,13 DiHOME was recently identified as an activator of transient receptor potential vanilloid 1 (TRPV1) (Green et al., 2016), loss of which is associated with decreased asthma prevalence in humans and protection against airway inflammation in animal models (Baker et al., 2016; Wang et al., 2009). To evaluate whether oxylipins delivered in the peritoneum reach the circulation, we quantified 12,13 DiHOME by liquid-chromatography mass spectrometry (LC-MS) (Gouveia-Figueira et al., 2017) three hours after injection and observed significant enrichment in both the plasma and lungs when compared with vehicle-treated animals (Figure 2h, Supplementary Figure 2i), indicating that 12,13 DiHOME may interact directly with lung tissue to exacerbate allergic airway inflammation.

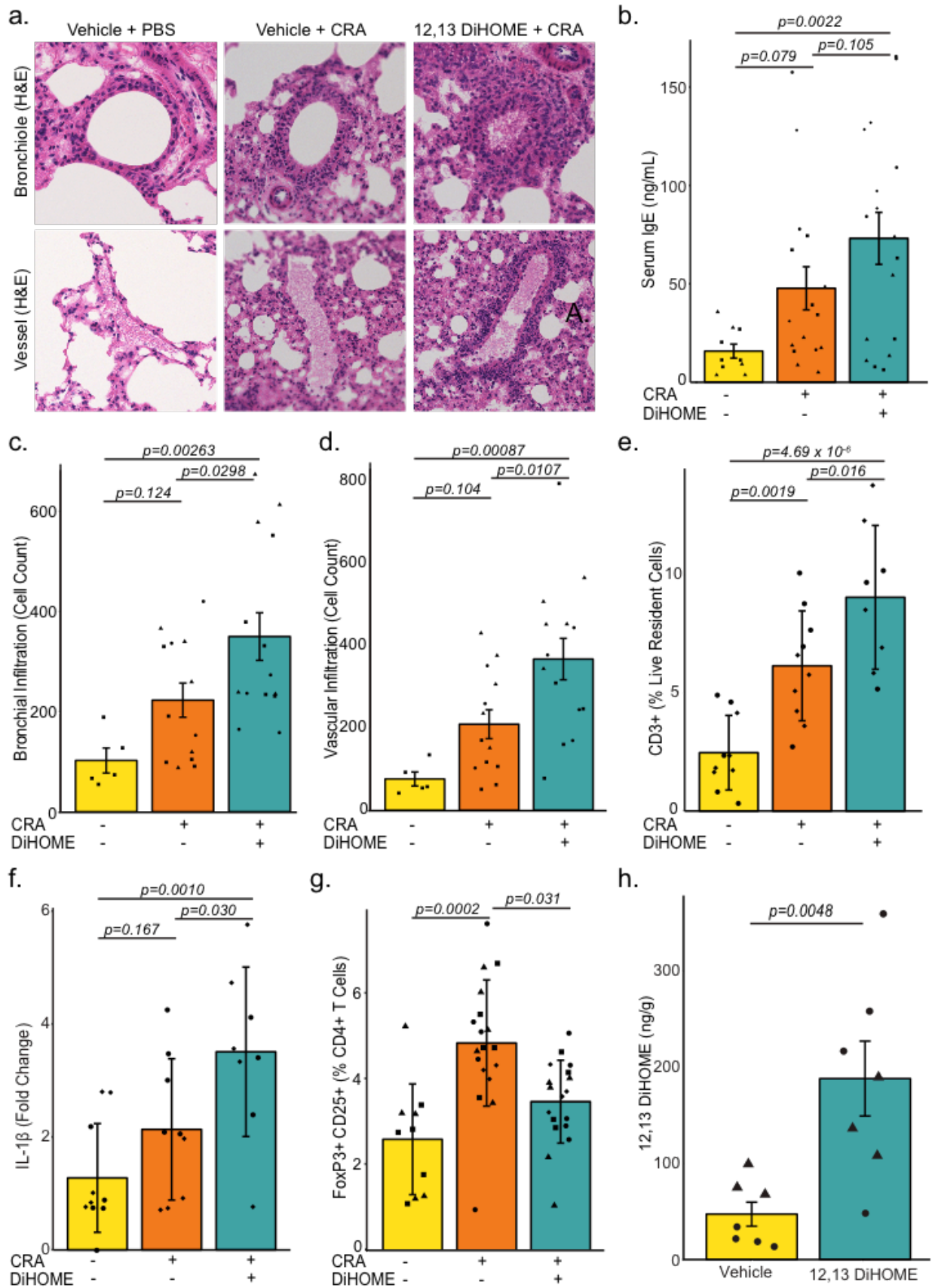


Figure 2: Peritoneal treatment with 12,13 DiHOME exacerbates lung inflammation in CRA-challenged mice. (A) Hematoxylin and eosin stained bronchioles and blood vessels from the lungs of mice treated with vehicle (10% DMSO) and challenged with PBS or CRA or treated with 30 mg kg⁻¹ 12,13 DiHOME (solubilized in 10% DMSO) and challenged with CRA. (B) Peritoneal treatment of mice with 12,13 DiHOME (n=17) increases serum IgE compared to CRA-challenged (n=16; LME; p=0.105) and PBS-challenged animals (n=10; LME; p=0.0022). (C,D) 12,13 DiHOME treatment (n=14) increases the number of infiltrating cells surrounding the bronchioles and veins of CRA-challenged mice compared with vehicle treated, PBS challenged [n=5; LME; p=0.00263 (bronchial), p=0.00087 (venous)] or vehicle treated, CRA challenged [n=13; LME; p=0.0298 (bronchial), p=0.0107 (venous)] animals. (E) Peritoneal 12,13 DiHOME treatment increases the frequency of lung resident T cells (CD3+) in CRA challenged mice (n=9) compared with vehicle treated, PBS challenged (n=10; LME; p=4.69x10⁻⁶) or vehicle treated, CRA challenged (n=10; LME; p=0.016) animals. (F) 12,13 DiHOME treatment (n=8) increases the expression of IL1 β compared with vehicle treated, PBS challenged (n=9; LME; p=0.0010) or vehicle treated, CRA challenged (n=9; LME; p=0.030) animals. (G) 12,13 DiHOME treatment of CRA-challenged mice (n=18) decreases Treg frequency compared to vehicle-treated CRA-challenged mice (n=18; LME; p=0.031). (H) Peritoneal treatment with 12,13 DiHOME significantly increases the concentration of 12,13 DiHOME in the lungs (n=6; two-sided student t-test: p=0.0048) at 3 hours post-delivery. Unique symbols (\blacktriangle , \blacksquare , \blacklozenge , \bullet) represent mice from independent assays. All error bars represent the SEM.

12,13 DiHOME is significantly enriched in the feces of neonates at risk of atopy and asthma

Given the apparent role of this lipid in driving pro-allergic immune dysfunction in mice and humans, we focused on determining the concentration and potential sources of 12,13 DiHOME in neonatal feces. We began by quantifying 12,13 DiHOME and 9,10 DiHOME (its enantiomer and a known agonist of PPAR γ (Lecka-Czernik et al., 2002)) using LC-MS in a subset of one-month-old neonates from the Wayne County Health, Environment, Allergy & Asthma Longitudinal Study (WHEALS; Table 1; total n=41; atopic=7; asthmatic=8; atopic asthmatic=4) (Fujimura et al., 2016). These included 26 one-month old stool samples that had been previously selected for untargeted metabolomic profiling based on their representation of the varied gut microbiome composition observed across 130 one-month old subjects (Fujimura et al., 2016) and an additional 15 randomly selected one-month old samples that had more than 50 mg of stool and 10 ng of extracted fecal DNA remaining and had childhood atopy and/or asthma outcomes available. 12,13 DiHOME was present in all neonatal stool, but was detected at significantly higher concentrations in the stool of neonates who subsequently developed

atopy and/or asthma (Figure 3a). In contrast the concentration of 9,10 DiHOME, an enantiomer of 12,13 DiHOME, did not significantly differ between the two groups (Supplementary Figure 3a).

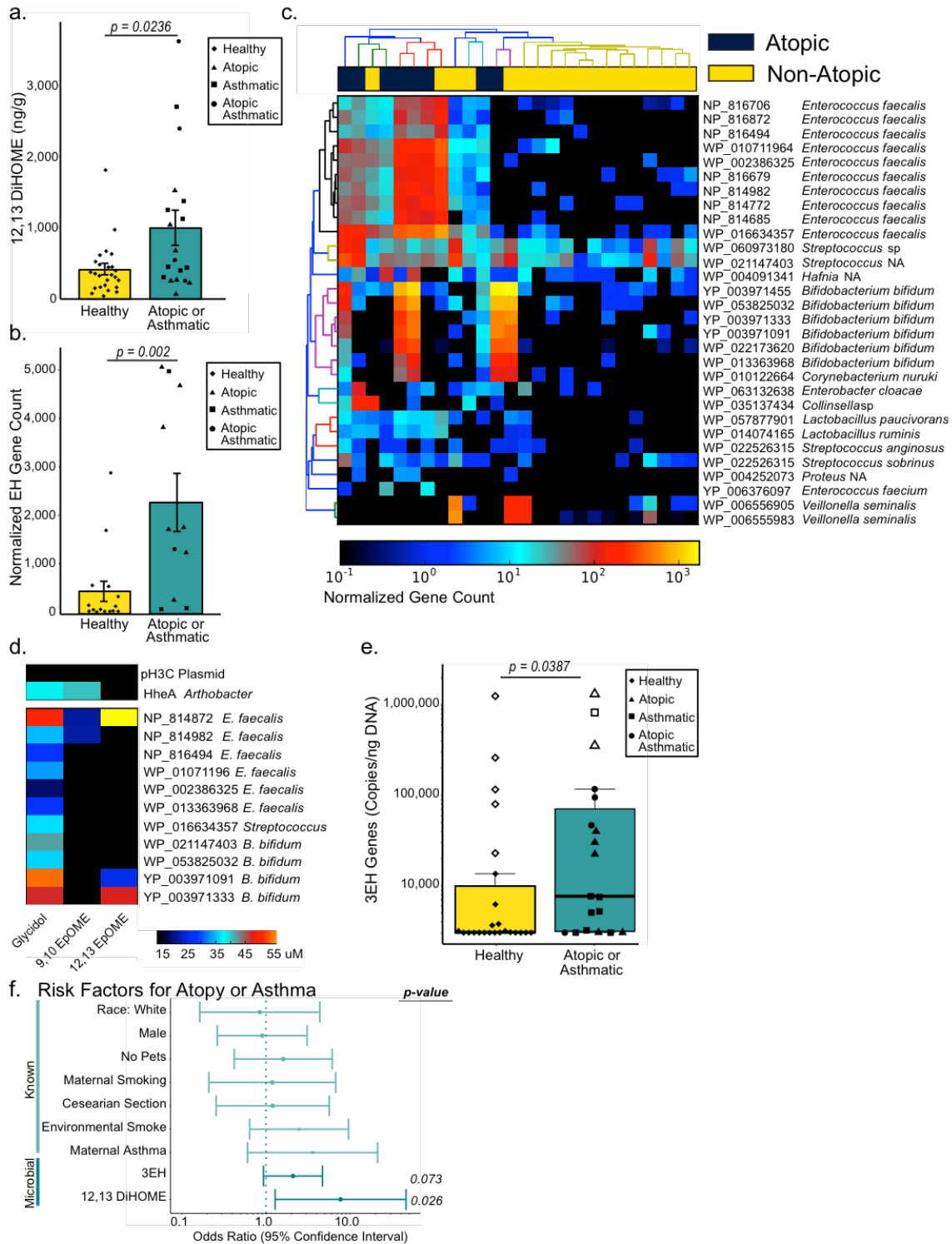


Figure 3: *Enterococcus faecalis* and *Bifidobacterium bifidum* strains in the neonatal gut microbiome encode the capacity to produce 12,13 DiHOME and increase the odds of developing atopy at age two or asthma at age four. (A) Neonates who develop childhood atopy and/or asthma exhibit increased fecal concentrations of 12,13 DiHOME (n=41; two-sided Wilcoxon test; p=0.0236). **(B)** Neonates who develop atopy at age two or asthma at age four have more bacterial EH genes in their stool (n=26; two-sided Wilcoxon test; p=0.002). **(C)** The 30 most

abundant EH genes identified in stool are enriched in neonates who develop atopy. **(D)** Three of the candidate EH genes, *E. faecalis* NP_814872, *B. bifidum* YP_003971091, and *B. bifidum* YP_003971333, convert 12,13 EpOME to its conjugate diol, 12,13 DiHOME. **(E)** 3EH copy number mimics the significant increase in overall fecal EH genes observed in neonates who go on to develop atopy and/or asthma (n=41; two-sided Wilcoxon test; p=0.0387, boxplot shows distribution of data on log-scale, open shapes represent potential outliers). **(F)** Increasing 12,13 DiHOME concentrations in neonatal stool significantly increased the relative odds of developing atopy at age two or asthma at age four, while increased 3EH copy number trended toward significance [n=41; Univariate Logistical Regression; 3EH (OR)=2.09; 95% confidence interval (CI)= 0.93-4.68; p=0.073; 12,13 DiHOME (OR)=7.67; 95% confidence interval (CI)= 1.28-46.0; p=0.026].

Specific Strains of *Bifidobacterium* and *Enterococcus* can produce 12,13 DiHOME

12,13 DiHOME is a terminal metabolic product of linoleic acid, which is initially converted to 12,13 EpOME either enzymatically via a cytochrome P450 epoxygenase (Ha et al., 2002) or spontaneously via oxidation (Mosblech:2009dq); 12,13 EpOME is then converted to 12,13 DiHOME via an epoxide hydrolase (EH); an enzyme encoded by humans, bacteria and fungi (Biswal et al., 2008; Decker et al., 2009; Morisseau, 2013). To identify potential sources of 12,13 DiHOME, the aforementioned 26 neonatal stool samples (Fujimura et al., 2016) underwent shotgun metagenomic sequencing. A database of known bacterial (~73,000), fungal (~5,000), and human (~50) EH genes was assembled and used in conjunction with ShortBred (Kaminski:2015bi) to probe the neonatal metagenomic data for sequence reads with EH homology. No fungal or human EH genes were detected; however, approximately 1,400 bacterial EH genes were identified. Bacterial EH genes were significantly more abundant in the stool of neonates who developed atopy and/or asthma (Figure 3b). The thirty most abundant of which were primarily encoded by *Enterococcus faecalis*, *Streptococcus*, *Bifidobacterium bifidum*, and *Lactobacillus* strains (Figure 3c).

To evaluate whether these putative EH genes are capable of hydrolyzing epoxides and producing 12,13 DiHOME, a cell-based assay was developed. A subset (n=11) of the most frequently detected putative bacterial EH genes, with $\geq 75\%$ of homologous EH marker regions identified in the metagenomic data, were selected (Table S1). These genes were synthesized and cloned into *Escherichia coli* for expression. EH activity was measured using modifications of

a previously described colorimetric assay (Fujimura et al., 2016). All 11 genes are capable of hydrolyzing glycidol, a generic epoxide, to its conjugate diol, glycerol, and three can hydrolyze 9,10 EpOME to 9,10 DiHOME. However, only NP_814872 (*E. faecalis*), YP_003971091 (*B. bifidum*), and YP_003971333 (*B. bifidum*) can convert 12,13 EpOME into 12,13 DiHOME (Figure 3d), indicating that while EH activity is common, the specific capacity to produce 9,10 or 12,13 DiHOME may be bacterial strain specific.

Strain-specific bacterial EH genes and their product, 12,13 DiHOME, are associated with the development of atopy and asthma in childhood

To test whether the three 12,13 DiHOME-producing bacterial EH genes (3EH) were sufficient to distinguish neonates who developed atopy and/or asthma in childhood from those who did not, we developed qPCR assays to quantify the 3EH copy number in neonatal stool. We measured fecal 3EH copy number in our subset of the WHEALS cohort and observed a significant increase in the stool of neonates who subsequently developed atopy and/or asthma in childhood (Figure 3e). Armed with these data we evaluated whether fecal 12,13 DiHOME and 3EH copy number were associated with increased odds of childhood atopy or asthma. Using our subset of the WHEALS cohort (n=41, Table 1) and univariate logistical regression, we examined the odds of developing atopy at age two years or asthma at age four years based on neonatal fecal 12,13 DiHOME concentration, fecal 3EH copy number, or known early-life risk factors selected *a priori* based on previously published literature. These included male gender; race; maternal asthma; lack of pets, maternal smoking, and environmental smoke exposure pre-delivery; delivery by Cesarean section; and formula feeding at one month (Bao et al., 2017; Burke et al., 2012; Gallant and Ellis, 2018; Havstad et al., 2011; Lodge et al., 2012; Wegienka et al., 2017; 2015).

Table 1: Comparison of sample characteristics for atopy at age two and asthma at age four. P values were calculated using a Fisher Exact test for all comparisons except age at the time of stool collection, which was calculated using a two-sided student T-test.

	Comparisons for atopy at age 2			Comparisons for asthma at age 4		
	Atopic (n=11)	Non-atopic (n=30)	P value	Asthmatic (n=12)	Non-asthmatic (n=29)	P value
Race						
White, no. (%)	1 (2.4)	6 (15)	0.651	2 (4.9)	5 (12)	1.000
Black, no. (%)	9 (22)	23 (56)	1.000	9 (22)	23 (56)	1.000
Male, no. (%)	4 (9.8)	16 (39)	0.484	6 (15)	14 (34)	1.000
Age of Stool, median (SD)	35 (4.24)	34.5 (21.5)	0.280	35 (14.3)	35 (20.5)	0.830
Maternal Asthma, no. (%)	3 (7.3)	4 (9.8)	0.361	3 (7.3)	4 (9.8)	0.398
Cesarean section, no. (%)	1 (2.4)	7 (17)	0.412	3 (7.3)	5 (12)	0.672
Exclusively Breastfed, no. (%)	1 (2.4)	3 (7.3)	1.000	0 (0)	4 (9.8)	0.302
Maternal Smoking, no. (%)	1 (2.4)	5 (12)	1.000	3 (7.3)	3 (7.3)	0.334
Environmental Smoke Exposure, no. (%)	3 (7.3)	10 (24)	1.000	6 (15)	7 (17)	0.146
No Pet Exposure, no. (%)	8 (20)	20 (49)	1.000	9 (22)	19 (46)	0.719

Univariate modeling indicated a significant increase in the odds of developing either atopy at age two years and/or asthma at age four with increased fecal 12,13 DiHOME, while increased fecal 3EH trended towards a significant increase (Figure 3f, Table S6). Multivariate modeling was used to test the remaining risk factors for potential confounding. There was no strong evidence for confounding in the relationship between 12,13 DiHOME or 3EH copy

number and the development of atopy at age two or asthma at age 4 (all changes in odds ratio < 20%). Clearly these neonatal gut microbiome risk factors require validation in additional larger cohorts. Nonetheless, they represent exciting targets for future study and potential intervention.

Material and Methods

Human Immune Assays

IL-10 secretion was measured using a cytometric bead array (BD Biosciences, San Jose, CA). Human DCs were isolated from the peripheral blood mononuclear cells (PBMCs) of two healthy human donors as previously described (Fujimura et al., 2016) and treated with increasing concentrations of 12,13 DiHOME (Cayman Chemical, Ann Arbor, MI) solubilized in 0.2% dimethylsulfoxide (DMSO). Supernatant was collected after 24 hours. IL-10 concentrations were determined according to the manufacturer's instructions.

Co-culture of human DCs and T cells in the presence of 12,13 DiHOME was performed as previously described (Fujimura et al., 2016). In brief, DCs were isolated from the PBMCs of two healthy human donors and treated for five days with 130 μ M 12,13 DiHOME solubilized in 0.2% DMSO or vehicle (0.2% DMSO) in the presence of 20 ng mL⁻¹ IL-4 (R&D Systems, Minneapolis, MN) and 10 ng mL⁻¹ GM-CSF (R&D Systems, Minneapolis, MN). Fresh treatment media was added every 48 hrs throughout the course of the study. Eighteen hours prior to co-culture, DCs were stimulated with 10 ng mL⁻¹ TNF α , IL1 β , and IL-6 (Peprotech, Rocky Hill, NJ) and 1 mM prostaglandin E2 (Stemcell Technologies, Cambridge, MA). DCs were subsequently washed and co-cultured with autologous T cells in the presence of 10 ng mL⁻¹ anti-CD28 and anti-CD49d (BD Bioscience, San Jose, CA).

After five days of co-culture, T cell subsets were analyzed by flow cytometry. To assess cytokine secretion, cells were stimulated for 16 hrs with Phorbol Myristate Acetate-Ionomycin (ACROS, Morris Planes, NJ) and GolgiPlug (Gplug; BD Biosciences, San Jose, CA). Antibodies used for staining are summarized in Table S2. Flow cytometry data was collected on a BD LSR

II flow cytometer. Helper T cell subsets were defined as follows: Th1 CD3+CD4+IFN γ +; Th2 CD3+CD4+IL-4+; Th17 CD3+CD4+IL-17+, Treg CD3+CD4+CD25+FoxP3+. The human T cell gating strategy can be found in Supplementary Figure 1d.

Human DC maturation was assessed by flow cytometry. PBMCs were isolated from two healthy human donors using Ficoll–Hypaque gradient centrifugation as previously described (Fujimura et al., 2016) and cultured for five days in the presence of 20 ng mL⁻¹ IL-4 and 10 ng mL⁻¹ GM-CSF. Monocytic DCs (DCs) were defined as CD3-CD19-CD11c+. The DC gating strategy can be found in Supplementary Figure 1e.

Gene expression was examined in human DCs. DCs were isolated as described above and treated for two days with 130 μ M 12,13 DiHOME. Cells were washed twice in PBS, and RNA was extracted using the RNAqueous™ Micro Kit (Ambion, Foster City, CA). The RT2 First Strand Kit (Qiagen, Germantown, MD) was used to synthesize cDNA, and expression of CD36, CD1a, FABP4, and HADH relative to beta-actin was measured using Power SYBR Green PCR Master Mix (ThermoFisher Scientific, Waltham, MA) and a QuantStudio 6 Real-Time PCR system (ThermoFisher Scientific, Waltham, MA). Primers are summarized in Table S3.

Luciferase Assay

A modified PPAR γ luciferase assay was performed as described in Ye et. al. (Ye et al., 2005). A PPRE-luciferase reporter plasmid, PPRE X3-TK-luc from Bruce Spiegelman (Plasmid # 1015; Addgene, Cambridge, MA), and a PPAR γ overexpression plasmid, pGST-PPAR γ from Bert Vogelstein (Plasmid # 16549; Addgene, Cambridge, MA), were purified with the Plasmid Plus Maxi Kit (Qiagen, Germantown, MD). Raw264.7 cells grown in R10 media [Roswell Park Memorial Institute (RPMI) media 1640 with 10% heat-inactivated Fetal Bovine Serum and 2 mM L-glutamine and 100 U mL⁻¹ penicillin–streptomycin] were transfected with the PPRE-reporter, PPAR γ , and Renilla luciferase plasmid DNA in a 1:20:40 ratio, using 50 ng per

well of reporter plasmid DNA. Fugene HD Transfection reagent (Promega, Madison, WI) was combined with plasmid DNA in a 4:1 ratio, and the total volume was brought to 5 μ L per well with RPMI. The transfection mixture was gently combined with dilute Raw264.7 cells and plated in black, clear-bottom, 96-well plates at a density of 50,000 cells per well. Twenty-four hours after transfection, cells were treated with 12,13 DiHOME, Rosiglitazone, or GW1929 (Cayman Chemical, Ann Arbor, MI) solubilized in 0.1% DMSO. Twenty-four hours after treatment Firefly luciferase and Renilla luminescence were measured using the Dual-Glo Luciferase Assay kit (Promega, Madison, WI) on a Cytation 3 plate reader (BioTek Instruments, Winooski, VT).

Animal Models

Six-week-old female C57B6 mice were obtained from Jackson Laboratories (Sacramento, CA). Mice were treated on days 1, 2, 3, 14, and 21 with 30 mg kg⁻¹ 12,13 DiHOME solubilized in 10% DMSO or vehicle (10% DMSO) by peritoneal injection. Three hours after injection, mice were challenged intra-tracheally with either PBS or CRA (20,000 PNU mL⁻¹; Greer, Lenoir, NC). Twenty-four hours after the final challenge mice were anesthetized, injected retro-orbitally with 100 μ L CD45-APC (1:10), allowed to recover from anesthesia, and subsequently sacrificed. Lungs and plasma were collected. Serum was isolated, and serum IgE levels were measured using a Mouse IgE ELISA Max kit (Biolegend, San Diego, CA).

Lungs were sent to the Mouse Pathology Core at UCSF for hematoxylin and eosin staining of paraffin-embedded tissue sections. Two bronchioles and two vessels from each stained tissue section were scored on a 0-4 scale with 0, representing structures with no inflammatory infiltrates; 1, representing few inflammatory cells; 2, representing a ring 1 cell-layer wide; 3, representing a ring 2-4 cells wide; and 4, representing a ring of inflammatory cells more than 4 cells wide. Each structure was scored by two blinded-individuals, and scores were averaged for each animal. Cell counts were determined for each structure. In brief, the ImageJ

freehand selection tool was used to trace the perimeter of each bronchiole and vessel. The area extending beyond the perimeter of the vessel was cleared, and the color threshold of the image was adjusted using the default method with the following parameters: hue=0-255, saturation=0-255, brightness=130-255, threshold color=white, background=dark, color space=HSB. The image was converted to an 8-bit grey scale, and the threshold was adjusted using the B&W defaults and a range of 0-150. Counts were outlined and summarized using the analyze particles window (size=0-infinity, circularity=0.0-1.00).

Lung cell subsets were assessed by flow cytometry. Lung tissue was manually dissected, digested with 5 mg per sample collagenase (Sigma-Aldrich, St. Louis, MO), and passed through a 40 μm filter to generate single cell suspensions. CD45- lung cells were considered resident cells and further classified as T cells (CD3+), neutrophils (Ly6G+ CD11b+), monocytes (F4/80+ Ly6C+ Ly6G- CD11b+), and alveolar macrophages (Siglec-F+ F4/80+ CD11c+ CD11b-). Gating strategy can be found in Supplementary Figure 2c. Regulatory T cells were identified as CD3+CD4+CD25+FoxP3+ cells, using the human T cell gating. A representative flow plot can be found in Supplementary Figure 2d.

Lung tissue was preserved in RNAlater (Ambion, Foster City, CA). Preserved lung tissue was homogenized in Lysing Matrix E Tubes using a FastPrep 24 Homogenizer (MP Biomedicals, Santa Ana, CA) and extracted using an RNeasy Mini Kit (Qiagen, Germantown, MD). Quantitative PCR was performed on lung tissue, as described above, to evaluate expression of IL1 α , IL1 β , and TNF relative to GAPDH. Primers are summarized in Table S3.

For quantification of 12,13 DiHOME in the lungs and plasma, six-week-old female C57B6 mice were purchased from Jackson Laboratories (Sacramento, CA) and treated with 30 mg kg⁻¹ 12,13 DiHOME solubilized in 10% DMSO or vehicle (10% DMSO) by peritoneal injection. Three hours after a single injection mice were sacrificed, and lung tissue and plasma were collected and frozen immediately in liquid nitrogen. 12,13 DiHOME was extracted from tissue and plasma using an established solid phase extraction protocol (Gouveia-Figueira et al.,

2015; Lundström et al., 2011). In brief, flash frozen tissue was massed and added to a Lysing Matrix E Tube (MP Biomedicals, Santa Ana, CA) containing 1 mL of methanol, 10 μ L 0.2 mg mL⁻¹ BHT/EDTA, and 1.25 ng 12,13 DiHOME-D4 (Cayman Chemical, Ann Arbor, MI) then homogenized as described above. Tissue samples were spun for 10 minutes at 2125 xg, and supernatant was transferred to a falcon tube containing 19 mL deionized water to generate a 5% methanol solution. Plasma samples were thawed on ice, and 10 μ L 0.2 mg mL⁻¹ BHT/EDTA and 1.25 ng 12,13 DiHOME-D4 were added to 250 μ L of thawed plasma. All samples were extracted using a Waters Oasis HLB Cartridges (60 mg of sorbent, 30 μ M particle size; Waters, Milford, MA) as previously described. Extracted samples were re-suspended in methanol, and LC-MS was performed on a Thermo LTQ-Orbitrap-XL mass spectrometer equipped with an electrospray ionization (ESI) source (ThermoFisher Scientific, Waltham, MA) as previously described (Gouveia-Figueira et al., 2017). Linear standard curves were generated using 6 injections of 12,13 DiHOME, 9,10 DiHOME, and 12,13 DiHOME-D4 (internal standard). Peaks were manually integrated, and recovery of the internal standard was used to correct for extraction efficiency. All mouse studies were reviewed and approved by the University of California San Francisco's Institutional Care and Use Program.

Study Population and Definitions

The original Wayne County Health, Environment, Allergy and Asthma Longitudinal Study (WHEALS) (Aichbhaumik et al., 2008) recruited pregnant women (n = 1,258) between the ages of 21 and 49 from August 2003–November 2007 in southeastern Michigan. Women were considered eligible if they lived in a predefined cluster of contiguous zip codes near Detroit, Michigan, had no intention of moving out of the area, and provided informed written consent. Follow-up interviews were conducted at 1, 6, 12, 24 and 48 months after birth. The 24-month appointment occurred at a standardized study clinic, where the child underwent evaluation by a

board-certified allergist. Stool samples from children were collected at one-month home visits and used in this study.

Samples were shipped to the University of California, San Francisco (UCSF), on dry ice, where they were stored at -80°C until processing. Fecal DNA extracted via the modified CTAB method(DeAngelis et al., 2009) and used for fungal and bacterial profiling was stored at -20°C for further analysis. Latent class analysis of blood drawn during the two-year clinic visit was used to define atopy as described by Fujimura et. al. and Havstad et. al. (Fujimura et al., 2016; Havstad et al., 2014). Asthmatic children were identified by parent-reported doctor diagnosis of asthma at the four-year interview. All research on human participants was reviewed and approved by the Henry Ford Hospital Institutional Review Board.

Neonatal Subset Characteristics

A subset of 41 neonates (median age=35 days) from the WHEALS cohort, that had previously undergone fecal fungal and bacterial profiling(Fujimura et al., 2016) and had more than 50 mg of stool and 10 ng of extracted fecal DNA remaining from the one-month home visits were selected (**Table 1**; total n=41; atopic=7; asthmatic=8; atopic asthmatic=4). These included 26 one-month old stool samples that had been previously selected for untargeted metabolomic profiling based on their representation of the varied gut microbiome composition observed across 130 one-month old subjects(Fujimura et al., 2016). To increase power, we also included an additional 15 randomly selected one-month old fecal samples from the WHEALS cohort that had more than 50 mg of stool and 10 ng of extracted fecal DNA remaining, and had childhood atopy and/or asthma outcomes available. Of the 41 samples in our subset 20 (48.8%) were male and 32 (78%) were black, based on a maternal report of race. Additionally, 8 (19.5%) were born by Cesarean section, 4 (9.75%) were exclusively breastfed until one month of age, 7 (17%) reported doctor-diagnosis of maternal asthma, 6 (14.6%) reported maternal smoking during

pregnancy, 13 (31.7%) reported household smoke exposure during pregnancy, and 13 (31.7%) lived with an indoor or outdoor dog or cat prior to delivery. The results presented in this study require replication in a larger neonatal population.

Mass Spectrometry in Human Samples

Fecal oxylipin (9,10 DiHOME and 12,13 DiHOME) concentrations were assessed in our subset of the WHEALS cohort (n=41). Oxylipins were extracted from approximately 50 mg of neonatal stool and quantified by LC-MS using the protocol described above. The concentrations of 12,13 DiHOME used in our *ex vivo* cell assays ($\sim 40 \mu\text{g g}^{-1}$) and *in vivo* animal models ($\sim 0.2 \mu\text{g g}^{-1}$) were within an order of magnitude of the concentrations measured in high-risk neonatal stool ($0.2\text{-}4 \mu\text{g g}^{-1}$).

Metagenomic Data Analysis

DNA from the 26 stool samples from the WHEALS cohort that had previously undergone untargeted LC-MS (Fujimura et al., 2016) and targeted oxylipin quantification (described above) was extracted using the modified CTAB method (DeAngelis et al., 2009) and sent to the Vincent J. Coates Genomic Sequencing Laboratory at the California Institute for Quantitative Biosciences for 150 base pair, paired-end sequencing on an Illumina HiSeq 4000 (www.qb3.berkeley.edu/gsl). Sequencing reads were quality-trimmed to Q17 with BBDuk (<https://sourceforge.net/projects/bbmap/>). A database of approximately 78,000 known bacterial ($\sim 73,000$), fungal ($\sim 5,000$), and human (~ 50) EH genes was generated using the NCBI protein database. All genes that had been tagged as “epoxide hydrolases” were included in the database. The EH database and the UniRef50 database (Suzek et al., 2015) were input into the ShortBred identify pipeline (Kaminski et al., 2015) and used to generate EH-specific markers. These markers were input into Shortbred quantify and were used to probe the quality-trimmed

metagenomes for EH markers. Normalized marker abundance for each gene was summed and used to generate the Normalized EH gene counts in Figure 3b. The thirty most abundant EH genes were visualized using a heatmap generated by HClust2 (<https://bitbucket.org/nsegata/hclust2>) and Canberra distance matrices (Figure 3c).

Colorimetric Detection of EH Activity

A subset of thirteen of the most abundant EH genes were selected for functional investigation based on the number of EH markers per gene identified in the metagenomic analysis (**Table S1**). Genes with fewer than 75% of markers were excluded from further analysis. The thirteen genes were structurally aligned with EH genes with known crystal structures from *Mycobacterium tuberculosis* (pdbid: 2bng), *Pseudomonas aeruginosa* (pdbid: 4dln), and *Rhodococcus erythropolis* (pdbid: 1nww) using the Promals3D server (<http://prodata.swmed.edu/promals3d/>) (**Supplementary Figure 5**). Amino acids extending beyond the EH domain were trimmed. Amino acid sequences were converted into DNA sequences using the default codon usage table for *E. coli* (http://www.bioinformatics.org/sms2/rev_trans.html), and restriction enzyme sites for EcoRI and Sall were added to the 5'- and 3'-ends of the DNA fragment, respectively. Genes were synthesized as gBlock gene fragments by IDT (<https://www.idtdna.com/>). Sequences of the synthetic constructs are summarized in Table S4.

Synthetic genes were sub-cloned into the EcoRI and Sall sites of a pH3C plasmid, graciously provided by Dr. Oren Rosenberg, to generate proteins with an N-terminal 8xHis fusion. Constructs were verified by forward and reverse sequencing of the T7 promoter (5'-TAATACGACTCACTATAGGG-3') and terminator (5'-GCTAGTTATTGCTCAGCGG-3') performed by Quintara Bio (Berkeley, CA). Eleven of the thirteen plasmids (NP_814872, NP_814982, NP_816494, WP_01071196, WP_002386325, WP_013363968, WP_01663157,

WP_021147403, WP_053825032, YP_003971091, YP_003971333) were validated and transformed into BL21(DE3) competent *E. coli* (New England Biolabs, Ipswich, MA) for expression. BL21 cells containing recombinant plasmids were streaked onto Lauria-Bertani (LB) agar plates supplemented with 50 $\mu\text{g mL}^{-1}$ kanamycin and grown overnight. Isolated colonies were selected and used to inoculate 200 μL LB supplemented with 50 $\mu\text{g mL}^{-1}$ kanamycin and 1 mM isopropyl- β -D-1-thiogalactopyranoside (IPTG; Sigma-Aldrich, St. Louis, MO).

Ninety-six well v-bottom plates containing inoculate were incubated for 18 hrs at 37°C at 200 rpm. Following incubation, plates were centrifuged for 10 minutes at 3000 rpm and washed with 20 mM HEPES pH 7.5. Cells were re-suspended, and 40 μL of re-suspended cells per well were added to 96-well flat bottom plates. The OD600 was measured to estimate protein concentration, and 40 μL of 13 mM epoxide was added to each well. Known concentrations of the conjugate diol plated in triplicate were included on each plate and used to generate standard curves (**Supplementary Figure 3b-d**). To each well, 20 μL of sodium nitrite was added (final concentration 20 mM). Plates were incubated for 1 hr at 37°C at 200 rpm. The reaction was stopped by centrifugation for 10 minutes at 4°C at 3000 xg. To a new 96-well flat bottom plate containing 50 μL 8 mM sodium periodate (final concentration 2 mM), 85 μL of supernatant was added. Plates were incubated for 30 min at room temperature while shaking. Background absorbance at 490 nm was recorded prior to the addition of 50 μL 12 mM adrenaline (final concentration 3 mM; Sigma-Aldrich, St. Louis, MO). Plates were incubated for 5 minutes at room temperature while shaking, and the absorbance at 490 nm was recorded. BL21 cells containing the pH3C plasmid or expressing HheA, a previously characterized EH(Tang et al., 2015), were included on each plate as controls. Enzymatic activity was assessed in triplicate for three epoxides, glycidol (Sigma-Aldrich, St. Louis, MO); 9,10 EpOME; and 12,13 EpOME (Cayman Chemical, Ann Arbor, MI), and their conjugate diols; glycerol, 9,10 DiHOME, and 12,13 DiHOME.

Quantification of 3EH Copy Number by qPCR

The abundance of the three active EH genes, NP_814872, YP_003971091, and YP_003971333, was quantified in fecal DNA extracted using the modified CTAB method (DeAngelis et al., 2009) from all 41 neonates. Gene fragments containing the target sequences (**Table S5**) were ordered from IDT (<https://www.idtdna.com/>) and used to generate a standard curve. In brief, gene fragments were amplified by PCR, normalized to 2×10^8 copies μL^{-1} , and eight 1:10 serial dilutions were made for use as standards. qPCR was performed using the TaqMan Universal PCR Master Mix (Applied Biosystems, Foster City, CA) and a QuantStudio 6 Real-Time PCR system (ThermoFisher Scientific, Waltham, MA). The 3EH copy number represents the total number of copies of all three genes per nanogram of fecal DNA. Sequences of gene fragments, primers, and probes are summarized in Tables S3 and S5.

Statistical Analysis

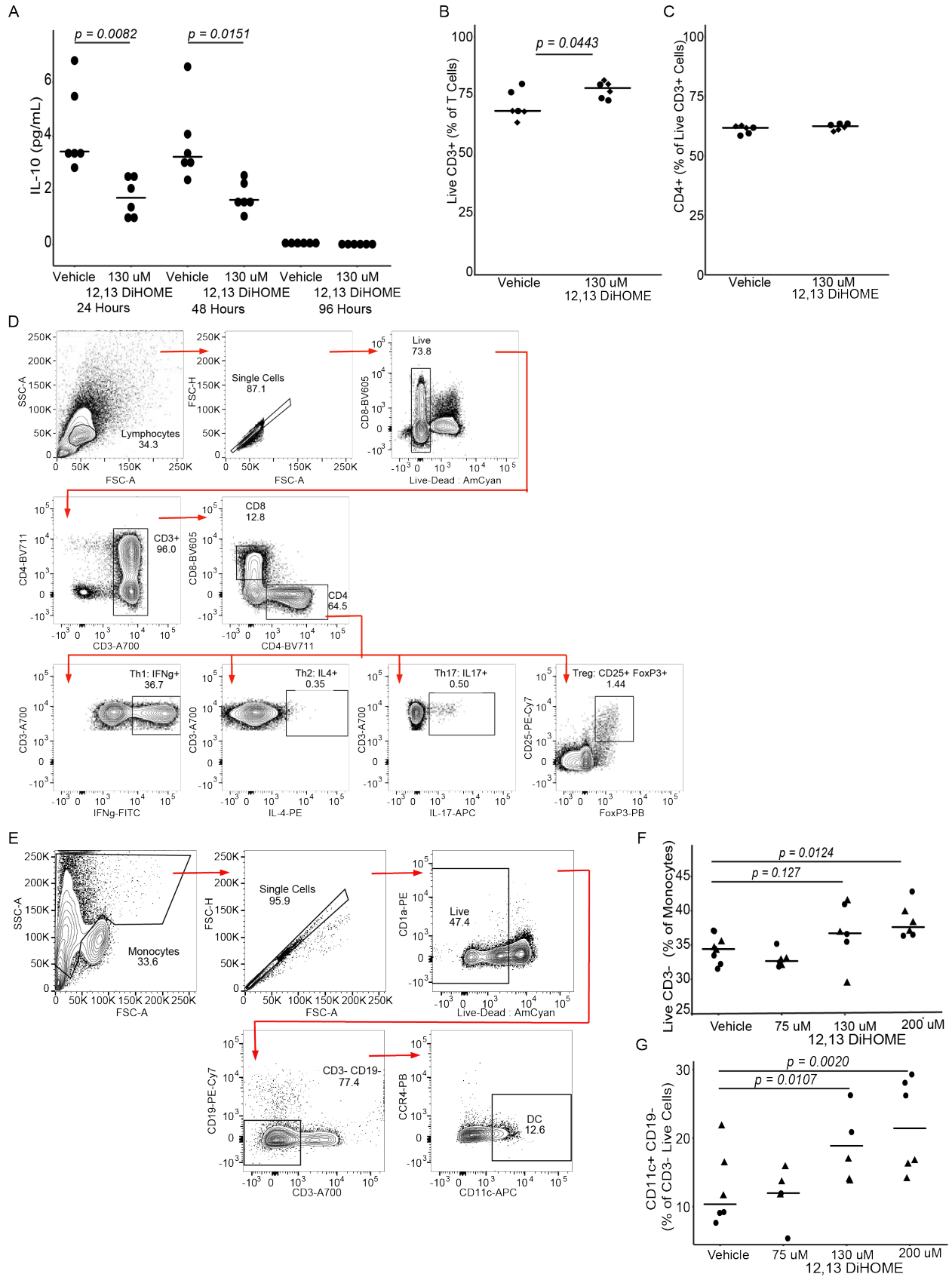
All analyses were conducted in the R statistical programming environment. All human cytokine, T cell, DC, and gene expression differences (**Figure 1, Supplementary Figure 1**) were tested using a linear mixed-effects model (LME; R package lmerTest) and adjusted for donors, with the exception of the distribution of autologous T cells (**Figure 1b**), which was tested using a multivariate analysis of variance (MANOVA). All comparisons made in mouse models (**Figure 2, Supplementary Figure 2**) were made using a LME with the exception of 12,13 DiHOME concentration (**Figure 2h, Supplementary Figure 2i**), which were compared using a two-sided student t-test. Fecal concentrations of 12,13 DiHOME and 9,10 DiHOME, normalized EH gene count, and 3EH copy number differences were tested using a two-sided wilcox rank sum test because a Shapiro test revealed that these data sets were not normally distributed.

Cohort characteristics were compared using Fisher Exact tests, with the exception of the age comparisons, which used a two-sided student T test (**Table 1**). Univariate logistical regression (logistical regression, R) was used to model the relationship between known risk factors (selected *a priori*), 3EH copy number, or 12,13 DiHOME concentration and the development of atopy and/or asthma in childhood (**Table S6**). Both 3EH copy number and 12,13 DiHOME concentration were log transformed before inclusion in the model because of the skew of the data (**Supplementary Figure 4a,b**). Risk factors selected *a priori* included race, gender, maternal asthma, maternal smoking pre-delivery, lack of pets pre-delivery, household smoke exposure pre-delivery, Cesarean delivery, and formula feeding at one month (Bao et al., 2017; Burke et al., 2012; Gallant and Ellis, 2018; Havstad et al., 2011; Lodge et al., 2012; Wegienka et al., 2017; 2015). Forest plots were created using odds ratios and confidence intervals determined by univariate logistical regression models (**Figure 3f**). Logistical regression was used to identify potential confounders of the statistically significant associations. Potential confounder were defined as risk factors that changed the adjusted odd ratios by >20%.

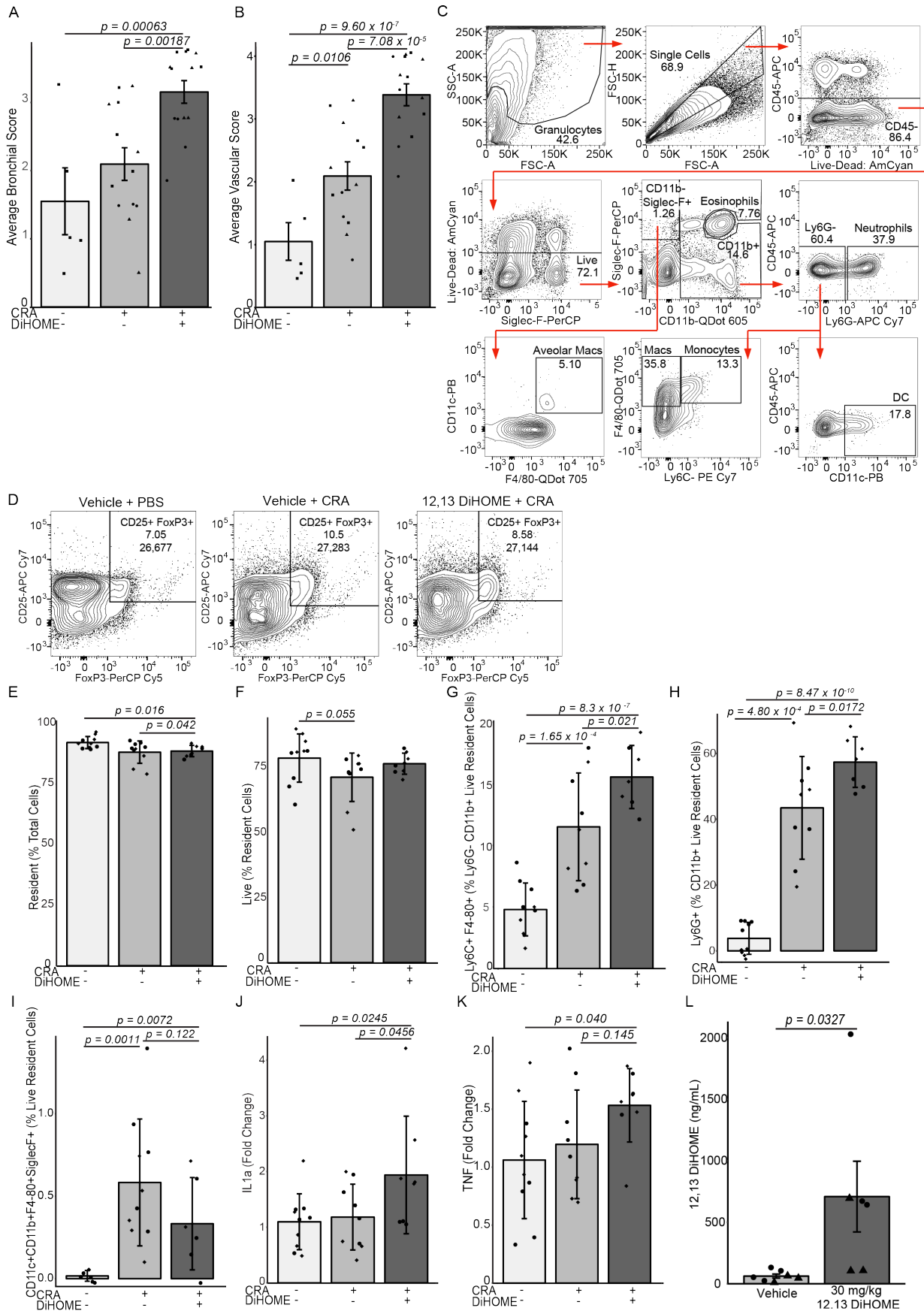
Data and materials availability

Metagenomic data generated in this study is available in the EMBL repository Accession # PRJEB24006 (<https://www.ebi.ac.uk/ena/>). Additional datasets and materials are available from the corresponding author upon request. Data sets and R scripts used for statistical analysis and figures are available on GitHub (<https://github.com/srlevan/>).

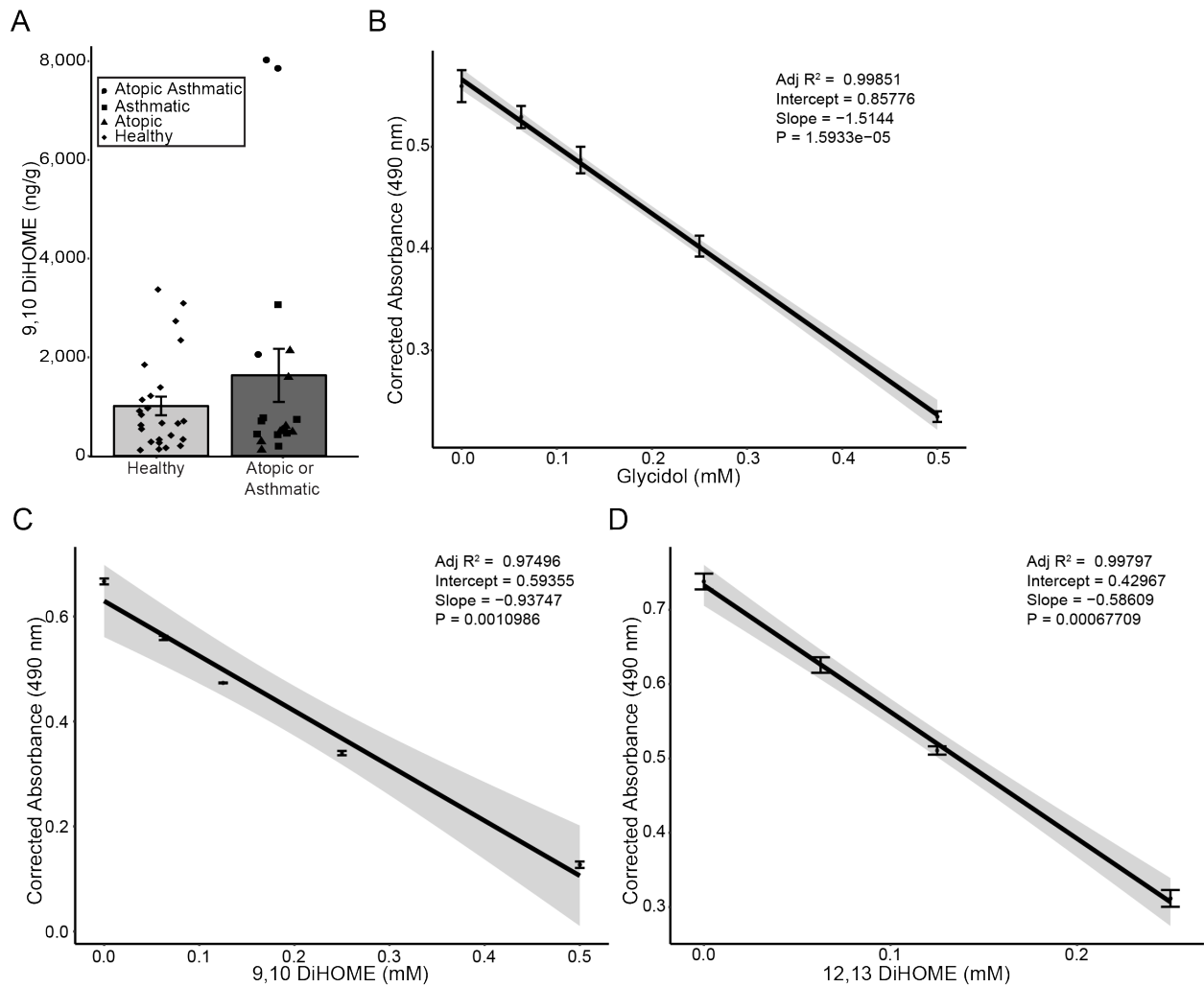
Supplementary Figures and Tables



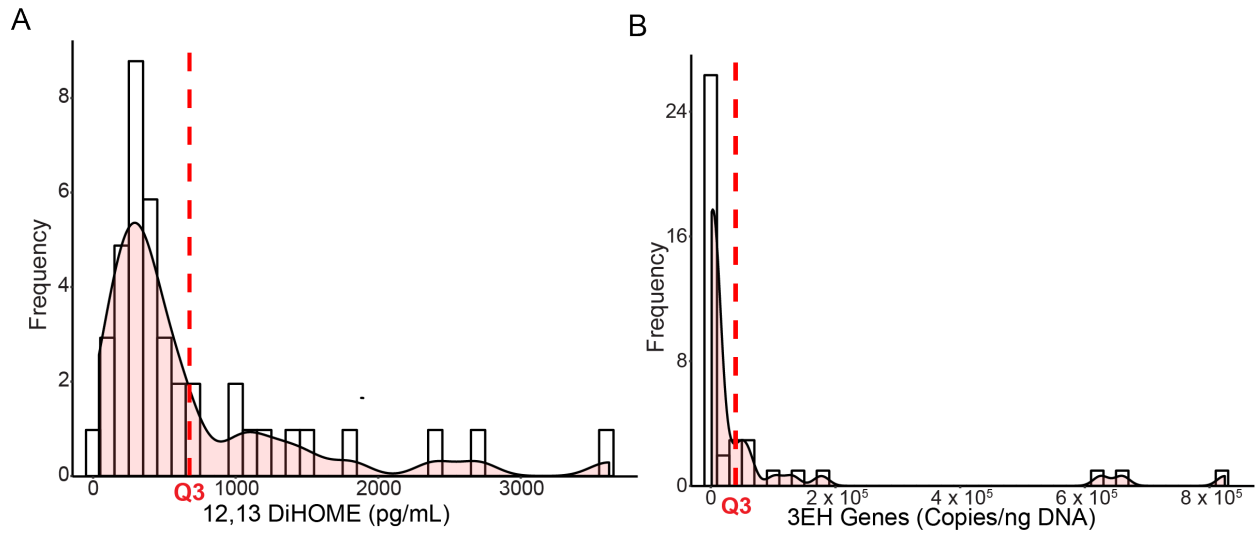
Supplemental Figure 1: 12,13 DiHOME treatment of DCs decreases IL-10 secretion and Treg frequency without affecting cell viability. (A) Treatment of DCs with 130 μ M 12,13 DiHOME causes significant decreases in IL-10 secretion 24 and 48 hours after treatment (n=3; biological replicates=2; LME; 24 hr p=0.0082; 48 hr p=0.0151). (B) Frequency of live CD3+ cells following co-culture with vehicle or 130 μ M 12,13 DiHOME-treated DCs (n=3; biological replicates=2 (u and ●); LME; p=0.0443) (C) Frequency of CD4+ T cells following co-culture with vehicle or 130 μ M 12,13 DiHOME-treated DCs (n=3; biological replicates=2 (u and ●)). (D) Gating strategy used to assess T cell subsets following co-culture of 12,13 DiHOME treated DCs with autologous T cells. (E) Gating strategy used to assess CD3- CD19- CD11c+ cells. (F) Frequency of live CD3- cells following PBMC treatment with vehicle or 12,13 DiHOME (n=3; biological replicates=2 (▲ and ●); LME; 130 μ M p=0.127; 200 μ M p=0.0124). (G) Frequency of CD3- CD19- CD11c+ live cells following PBMC treatment with vehicle or 12,13 DiHOME (n=3; biological replicates=2 (▲ and ●); LME; 130 μ M p=0.0107; 200 μ M p=0.0020).



Supplemental Figure 2: Peritoneal treatment with 12,13 DiHOME exacerbates innate immune infiltration in the lungs of CRA-challenged mice. (A,B) Peribronchial and perivascular infiltration were scored in H&E stained lung sections (0 - no inflammatory infiltrates; 1 - few inflammatory cells; 2 - ring 1 cell-layer wide; 3 - ring 2-4 cells wide; 4 - ring > 4 cells wide). 12,13 DiHOME treatment (n=14) increases the peribronchial and perivascular inflammation score compared to vehicle treated, PBS challenged [n=5; LME; p=0.00062 (bronchial), p=9.60x10⁻⁷ (venous)] or vehicle treated, CRA-challenged [n=13; LME; p=0.00187 (bronchial), p=7.08x10⁻⁵ (venous)]. **(C)** Gating strategy used to assess resident immune cells in mouse lungs. **(D)** Representative flow plots displaying lung Tregs in mice (FoxP3+CD25+CD4+CD3+). **(E)** 12,13 DiHOME treatment of CRA-challenged mice (n=7) decreases the frequency of resident lung cells compared to vehicle treated, PBS challenged (n=9; LME; p=0.016) or vehicle treated, CRA challenged animals (n=9; LME; p=0.042). **(F)** 12,13 DiHOME treatment of CRA-challenged mice (n=7) does change the frequency of live resident cells in the lungs (vehicle treated, PBS challenged n=9; vehicle treated, CRA challenged n=9). **(G)** 12,13 DiHOME treatment of CRA-challenged mice (n=7) significantly increases the frequency of lung resident monocytes (Ly6C+F4-80+Ly6G-CD11b+) compared to vehicle treated, PBS challenged (n=9; LME; p=8.3x10⁻⁷) or vehicle treated, CRA challenged animals (n=9; LME; p=0.021) **(H)** 12,13 DiHOME treatment of CRA-challenged mice (n=7) significantly increases the frequency of lung resident neutrophils (Ly6G+CD11b+) compared to vehicle treated, PBS challenged (n=9; LME; p=8.47x10⁻¹⁰) or vehicle treated, CRA challenged animals (n=9; LME; p=0.0172). **(I)** 12,13 DiHOME treatment of CRA-challenged mice (n=6) decreases the frequency of lung resident alveolar macrophages (CD11c+CD11b+F4/80+Siglec-F+) compared to vehicle treated, CRA challenged animals (n=6; LME; p=0.122) but increases the frequency compared to vehicle treated, PBS challenged animals (n=6; LME; p=0.0072). **(J,K)** 12,13 DiHOME treatment increases the expression of IL1 α and TNF in 12,13 DiHOME treated, CRA challenged mice (n=8) compared to vehicle treated, PBS challenged [n=9; LME; p=0.0245 (IL1 α), p=0.040 (TNF)] or vehicle treated, CRA challenged animals [n=9; LME; p=0.0456 (IL1 α), p=0.145 (TNF)]. **(L)** Peritoneal treatment with 12,13 DiHOME significantly increases the concentration of 12,13 DiHOME in plasma (n=6, two-sided student t-test: p=0.0327). Unique symbols (\blacktriangle , \blacksquare , \blacklozenge , \bullet) represent mice from independent assays. All error bars represent the SEM.



Supplemental Figure 3: Bacterial EH enzymes can generate 9,10 and 12,13 DiHOME *in vitro*. (A) The fecal concentration of 9,10 DiHOME did not significantly differ between healthy neonates and those who develop atopy and/or asthma (n=41). The following symbols, u, ▲, n, ●, represent neonates who develop into healthy, atopic, asthmatic, and atopic asthmatic children, respectively. Error bars represent the SEM. (B,C,D) Calibration curves generated using a modified colorimetric assay for glycidol, 9,10 DiHOME, and 12,13 DiHOME, respectively. Error bars represent the standard deviation. Best-fit curves were generated using the lm (linear modeling) function in R.



Supplemental Figure 4: The distributions of 12,13 DiHOME concentration and 3EH copy number were skewed in our subset of hte WHEALS cohort (n=41). (A,B) Fecal concentrations of 12,13 DiHOME and 3EH copy number exhibited a right-skew.

Supplemental Figure 5: Alignment of thirteen EH candidate genes with *Mycobacterium tuberculosis* (pdbid: 2bng), *Pseudomonas aeruginosa* (pdbid: 4dlh), and *Rhodococcus erythopolis* (pdbid: 1nww), the crystal structures of which have been solved. Alignment was performed using Promals3D. The keys for consensus amino acid symbols (consensus_aa) and consensus secondary structure symbols (consensus_ss) can be found at <http://prodata.swmed.edu/promals3d/info/consensus.html> and http://prodata.swmed.edu/promals3d/info/consensus_ss.html, respectively.

Supplemental Table 1: Conserved marker regions for the top differential EH genes found in the metagenomic sequencing data. Fold changes were calculated comparing neonates who developed atopy to those who did not. P-values were generated using a two-sided Wilcoxon test and adjusted using the Benjamini & Hochberg (BH) correction. The frequency of conserved markers found in the metagenomic data were used to select candidate genes for further analysis.

Gene	Taxa	Fold Change	Adjusted p-value	Markers	% Markers
NP 814685	<i>Enterococcus faecalis</i>	4.79	0.0237	3 of 4	75%
NP 814772	<i>Enterococcus faecalis</i>	3.85	0.0237	5 of 6	83%
NP 814872	<i>Enterococcus faecalis</i>	4.03	0.0237	4 of 5	80%
NP 814982	<i>Enterococcus faecalis</i>	3.92	0.0237	5 of 6	83%
NP 816494	<i>Enterococcus faecalis</i>	4.12	0.0237	2 of 2	100%
NP 816679	<i>Enterococcus faecalis</i>	3.73	0.0237	4 of 6	67%
NP 816706	<i>Enterococcus faecalis</i>	4.45	0.0237	3 of 5	60%
WP 002386325	<i>Enterococcus faecalis</i>	3.29	0.0237	6 of 7	86%
WP 010711964	<i>Enterococcus faecalis</i>	3.9	0.0237	6 of 7	86%
WP 016634357	<i>Enterococcus faecalis</i>	4.21	0.0237	14 of 15	93%
WP 021147403	<i>Streptococcus</i>	2.16	0.042	7 of 9	78%
WP 060973180	<i>Streptococcus</i> sp	2.17	0.038	4 of 6	67%
WP 010122664	<i>Corynebacterium nuruki</i>	5.33	0.0131	1 of 7	14%
WP 013363968	<i>Bifidobacterium bifidum</i>	5.05	0.004	1 of 1	100%
WP 022173620	<i>Bifidobacterium bifidum</i>	5.39	0.0253	1 of 3	33%
WP 053825032	<i>Bifidobacterium bifidum</i>	5.2	0.0262	6 of 6	100%
YP 003971091	<i>Bifidobacterium bifidum</i>	6.82	0.0185	3 of 3	100%
YP 003971333	<i>Bifidobacterium bifidum</i>	4.87	0.0393	5 of 5	100%
YP 003971455	<i>Bifidobacterium bifidum</i>	4.92	0.0028	9 of 13	69%
WP 035137434	<i>Collinsella</i> sp	2.52	0.0422	4 of 6	67%
WP 063132638	<i>Enterobacter cloacae</i>	7.33	0.0095	4 of 6	67%
WP 014074165	<i>Lactobacillus ruminis</i>	2.62	0.0093	1 of 9	11%
WP 057877901	<i>Lactobacillus paucivorans</i>	2.57	0.009	1 of 7	14%

Supplemental Table 2: Antibodies used for human and mouse immune cell staining.

Human T Cell Panel			
Antibody	Clone	Vendor	Dilution
anti-CD4	L200	BD	1:100
anti-CD25	M-A251	BD	1:25
LIVE-DEAD Aqua		Life Technologies	1:300
anti-CD3	SP34-2	BD	1:100
anti-FoxP3	PCH101	eBioscience	1:20
anti-IFNg	B27	BD	1:200
anti-IL4	7A3-3	Miltenyi Biotec	1:20
anti-IL-17	64DEC17	eBioscience	1:20
Human DC Panel			
Antibody	Clone	Vendor	Dilution
anti-CD11c	B-ly6	BD	1:50
anti-CD19	SJ25C1	BD	1:100
LIVE-DEAD Aqua		Life Technologies	1:300
anti-CD3	SP34-2	BD	1:100
anti-CCR7	3D12	BD	1:35
anti-CD80	2D10	Biolegend	1:50
anti-CD86	2331	BD	1:50
anti-HLA-DR	G46-6	BD	1:50
anti-CD36	CB38	BD	1:50
Anti-CD1a	HI149	BD	1:40
Mouse T Cell Panel			
Antibody	Clone	Vendor	Dilution
anti-CD4	RM4-5	BD	1:100
anti-CD25	PC61	BD	1:50
LIVE-DEAD Aqua		Life Technologies	1:300
anti-CD3e	500A2	BD	1:150
anti-FoxP3	FJK-16s	eBiosciences	1:70
Mouse Innate Panel			
Antibody	Clone	Vendor	Dilution
anti-CD11b	M1/70	Biolegend	1:100
anti-CD11c	N418	Thermofisher Scientific	1:100
LIVE-DEAD Aqua		Life Technologies	1:300
anti-CD45	30-F11	Thermofisher Scientific	1:10
anti-SiglecF	E50-2440	BD	1:100
anti-F4/80	BM8	Biolegend	1:100
anti-Ly6c	AL-21	BD	1:100
anti-Ly6g	1A8	Biolegend	1:100

Supplemental Table 3: Primers used for human, mouse, and bacterial qPCR.

Human qPCR Primers		
Gene	Primer	Sequence
HADH	Forward	ATCAACACTGCCAGTGTGGCT
HADH	Reverse	AGTGTCATGCCCACTATTCCC
FABP4	Forward	GGATGGAAAATCAACCACCA
FABP4	Reverse	GGAAGTGACGCCTTTCATGA
CD1a	Forward	ACCTGTCCTGTCTGGGTGAA
CD1a	Reverse	CCCACGGAAGTGTGATGCT
CD36	Forward	TCTTTCCTGCAGCCCAATG
CD36	Reverse	AGCCTCTGTTCCAAGTATAGTGA
Beta-actin	Forward	AAGATGACCCAGATCATGTTTGAGACC
Beta-actin	Reverse	AGCCAGTCCAGACGCAGGAT
Mouse qPCR Primers		
Gene	Primer	Sequence
IL1a	Forward	CGAAGACTACAGTTCTGCCATT
IL1a	Reverse	GACGTTTCAGAGGTTCTCAGAG
IL1b	Forward	GAAATGCCACCTTTTGACAGTG
IL1b	Reverse	TGGATGCTCTCATCAGGACAG
TNF	Forward	CCCTCACACTCAGATCATCTTCT
TNF	Reverse	GCTACGACGTGGGCTACAG
GAPDH	Forward	CCTCGTCCCGTAGACAAAATG
GAPDH	Reverse	TCTCCACTTTGCCACTGCAA
Bacterial EH qPCR Primers and Probes		
Gene	Primer	Sequence
NP_814872	Forward	CGA CGG AAC ATT GCT AAA TTC AC
NP_814872	Reverse	CAA AGG ACG GCC TGT ACA TAA
NP_814872	Probe	/56- FAM/ACGGGTCAA/ZEN/AGAAGCGCTCCAAA/3IABkFQ/
YP_003971091	Forward	GTC GTT CAG ACG CAA CCA TA
YP_003971091	Reverse	TTT GTG GCC GGG ATT GTT
YP_003971091	Probe	/56- FAM/TACTATGCG/ZEN/GACAAGGCGGTGTTTC/3IABkFQ/
YP_003971333	Forward	GCA CCG ACC GTG AAC AT
YP_003971333	Reverse	GGA CAG CTT CGC TTC ATC TT
YP_003971333	Probe	/56- FAM/CGCTGAAGC/ZEN/ATGAGACGTTCCAGA/3IABkFQ/

Supplemental Table 4: Sequences of the synthetic EH gene constructs used in the *in vitro* screen on EH activity.

Synthetic Epoxide Hydrolase Genes	
Gene	Sequence
NP_814685	aattgcagaattcatgattaactgattgagcgatggatggcaccctgctggat gcgaaaatgagcattaccaacgataacgagcgcgattcggaagcggaaacgc ctgggcattgaattatggtggcgaccggccgcgctataccgaagcgaaccggc gctggaagaagcggcattgattgagcgatgattaccctgaacggcgcgaggtgt ttgataaagatggccatagcctgtttaccgcgggcattgaaaaagaaaccgtgacc gaagtgctgaccattctgagccagcataacgtgtattatgaaattgacccaacaaa ggcatttttagcgaacatcaggaaaaacgattgaaaactttgcggcgatattgag gaaagcatgccgatctgacctataaagtggcgattgagatggcgagcgcgatct gagcctgctgcatattacctatgtggatcgctggatgatattctgaaagatgatagca ttgaagtctgaaaattattggcttttagcatggatggcccgaagtgtggcccggc gggcatggaagtggaagaactggatgatctggtggtgaccagcagcgcgtaac aacattgaaattaaccatcgctggcgagaaaggcattgctggtggcgcgctggc gaaagaacgcgcatccggcggaacaggtgatgaccattggcgataacctgaa gatgtgagcatgattcagtgggcgggcgtagctttgagatgggcaacgcggaact ggaactgaaagaatgagcaaatatgaaaccgagaccaacctgaaaacggcgt ggggaagcgattctgagcgatcgcggaagatctggtgtcgactatccggcc
NP_814772	aattgcagaattcatgaaaaactgattgagattgatctggatggcaccacctgaa cgcgagagcctgattagcccgaaccgaacagaccctgaaaaagcgattga taacggccattatgtgagcattgagaccggccgcccgtatcgatgagccatcagttt tatcagcagctggcctgaccacccgatggtgaacttaacggcgcgctggtgcat attccggaaaaaaatgggatctggaagcgaagcgaacattgaaacgagatctgg tgttgatattctggcgagaaaaagaactgagctgattttgtggcgcgaaaa caaagaaacctttatattgataacctggatggctttgatccgaaatttttgagcaa agcgacctggataacctgctgaccgcaaaaaactgagcaccacccgaccag catgatggtgagcaccacccgaaccaggcggaagtggggataacctgac caaacgatgagcattatattgatgtgagcaccctggggcgcccgatgagcattctg gaaatggtggcgaaggcattcagaaagcgatggcgatgaggtggcgaact ttctgagcgtgaaaccggcgatattattgctttggcgatgaacataacgatgaaga aatgctgagctatgagggctggggcggtggcgatgaacaacgagaccgataaaatt aaaagcgtggcgaacgatgtgaccgaaaaaaccaacgatcaggatggcctggc ggattatctggaactatctggatctggtgtcgactatccggcc
NP_814872	aattgcagaattcatgagcattaaactggtggcgattgatattgatggcaccctgctga acagccagcataaaattacccgagcgatgaaagaagcgtgcagaaagcgaac gaacagggcgctgagcattgtgctgaccggccgcccgtgcccggcgtaag aacagctggatgaactggcgctgatggcgaaaacgattttgtgattacctataacgg cagcctggtgagggcgaccaagataacaccattatgaccgctataacctgagct atgaagattttctgaaattgaaatgtatagccgcaaagtggggcgcgatctgcatac cattgatgatagcagcattataccggaaccgcaacattggcaaatataccattcat gaagcgagcctggtgaacatgcccgtgaaatctgaccggtgatgaaatgacc cggaaatgaacattataaaatgatgatgattgatgaaccggaagtgtgattccgg cgattgcaaaactgcccgtgattttaccgaaaaatataccacctgaaaagcacc ccgttttattatgaaattatgacaaaaacgagcaaaaggcaacgctggcgaa actggcgatcatctggcctgaacaaagatgaagtgatggcgattggcgataacg aaaacgatctgagcattgattatgctggcattggcgtggcgatgggcaacgag accgaaaacgtgaaaaccattgaggatgtgataccaccagcaacgatgaagatg gcgtggcgagattatgaaaaatggtgctgattgtgtcgactatccggcc

NP_814982	<p>aattgcagaattcatggataaaatgaaagcgattacctttttgatctggatggcacct gctggatggcaccagccagattacccccgaaattaccgaggcggtggcggcgctg aaagataaccagattctgccgctgattgacgaccggccgaccctgtgcgaaattca gccgattatgaaagcgagcggcattgatagcgcgattgtgatgaacggccagttatt cattatgaaggcaaaaccattatagcgatgaattaccaccgaagaatgctgagc ctgcatgaacatgtgaaacagcgcggccatgaactggcgtttataacgaacgccg catttttgcaccggccataaccggcaccgtgaaacagcgatgattatattcatagcg cggtgccggaaattgatccgaccggctatgaaaacgatgagggtgaaatgatgctg gtgctgagccagcatggcgatgatgatgaatattattatgaacgctttccggaactga cctttatcgcaacggcccgttagcattgatattgtgcgcaaaaggcgtgagcaaagg cagcggcgtgaaaaacctgttaaacacctggcctgaacggcattccgacctatgc gtttggcgatggcattaacgatctggcgctgtttgaagcgtgagcattatggcattgcat gggcaacgcgcgcaagaactgaaagaaaaagcgaccttatttagcaccaaaa acaccgaaaacggcattgtgaacggcctgaaaaattgatctgctggtgtcgactt atccggcc</p>
NP_816494	<p>aattgcagaattcatgaaagcgggtgctgaccgatctggataacacctgattgctg gaacaaccggatggcaccgaagaactgaaaacctggctgctggaatgaaaa acgcgggcattaccgtgctggtggtgagcaacaacaagatagccgattaaacg cgtggtggaaaaaattgatctggattatgtggcgcgcgcgctgaaaccgaccgcgcg cggcittaaactggcggaaaaaaaactggcctgaaaccgagcgaatgctgatg gtggcgatcagattatgaccgatattcgccggcgaacgcggcggcattcgcaa cgtgctggtgcagccgattgtggataccgatggctggaacaccgcattaaccgcttt ttgaaacgcaaaattatgaaatatctgagcaaaaaagtgtcgacttatccggcc</p>
WP_01071196	<p>aattgcagaattcatggcgggtgaaagcattgtgatggatattgatggcacctgctg accagcgaaaaaaaaaattagcccgaaaaccggccaggcgtggtggcggcgca gaaacagggcctgagcctgattctggcgagcggccgcccgaccaaccgcatgcg cccgtggcggatgaaactggaaatggcgcattataacggccatctgctgagctata cggcgcgtgctgacccatcatggcagccagcagcagctgttaaccagaccatta gaaaagcctgagccagcagattctggaacatctgaaacagtttgatgtgattccga tgattaacgatgaaacctttatgtatgtgaaacgatgtgttcataaacacctgcatctgg aaaccggcatttaacattatgaaatgaaagccgcggcggcaactttcagctgtg cgaatggcatgatctggcggcgcctgaactttccgctgaacaaaattctgattgcg ggcgaaccggcgtatctgcagaaatatcatgaagcattatgcccgtttaaagaa accgtgaccgcggcgttagcgcgcgctttttttgaattaccgcgaaaaacattgat aaagcgcgcagcctggaaaaaactgacctgcagctgggcattaccgcggaagaa gtgattgcgtttggcgatggccataacgattataccatgctggaatggcggggcacc ggcattgcatggaaaacgcgggtggatgaaactgaaaaacattgacgaccgaagtga ccctgagcaacgataacgatggcattgctggtggcgtggcgaaaattgtggcgctt gtcgacttatccggcc</p>
WP_002386325	<p>aattgcagaattcatgctggaagcagcgaagtgaaaatgtatcagaccattctgttt gatctggatggcaccattaccgatagcggcagcggcattatgcgagcattctgtatg cgaccgaacagctgggctggccggcggcagcgaagaaacctgctgcagctttat tggcccgcgctgatgaaagctttctgcatatggcgcgagcgcggaagcggcgc agcaggcgggtggccattatcgcgctattatcagcgcgaaaggcatgtttgaaacc atgtgatccgggcatccggaagtgtgaccgcctgaaagaagcgggcgcgaa actgtatattgcgaccagcaaacgggaagaattgcaaaaaaattattaccatttt gatctggatcgctattttaccggcatttatggcgcgagcattgatggccatcgagca aaaaagcggatgtgattcagatgctgctgaccgaagcgcagctggatccgaccaa agaagcattattatggtggcgatcgcaaccatgatattctgggcgcgagcaga acggcctggatagcattggcgtgctgatggctttggcgaagaaaccgaactgcag gaagcgggcgagacctttctgtgagcagcccgaagatctgggcgagcttctgct</p>

	gcagaacagcgtgtgcacttatccggcc
WP_013363968	aattgcagaattcatgacccgcatgctgtttctggatattgatggcaccctggtgggca aagatcagcgcattccgcagagcgcgattcgcgcgattcgcgcggcgaggga acggccatctggtgctgattgcaactggtcgtgctcgcgcgggtgcggcaggctggc gftatgcgctgcgtccgggcgctggcagcaggccgcggcaccgcgttctgctgc ggccatcatggccgcgcggcgccgcatggcggcgatcgccagcgcgcaag gtgtgcacttat
WP_016634357	aattgcagaattcatgtatagcattgaaaccctggcgcgcatgtggataccctgtgctg ataaaaccggcaccattaccgaaggcaaatgaaagtgcagaaagcgattattct gcatgataaatatgaagaactgttccgcagattattggcagctatctgagcgaagc accgataacaacattaccatgcaggcgattcgcgatcattatgaagtgcgaaccg ctttggcgcgaaagaagtgtgctggcgttagcagcgaacgcaaatggggcgcgattg aattccggaattggcaccgctgtatctgggcgcgcgggaacgcctgggtgatgata gccgctgcccgaagcgggtttaccgcgcaggaaaacggctatcgcgtgctgatg ctggcgattgcggaacagcagccgctgaacgaaacaaaatgccgatctggaac cgctggcgattctggaattgatgatccgattcgcgagaacgcgaaagaaccctg gctgtatgaaagaagaaggcattgatctgaaagtattagcggcgataaccgggt gaccgtgagcaacattgcgcgcgcggcctgccgggctatgaaagctatattg atctgagcaccaaaaccaccgaagcggaaagtgcgcaagcgggtgcagcagata ccgtgttggccgctgagcccgcagcagaacgcaccattgtgcgcaactgaa agataccgaacatgtggtggcgatgaccggcgatggcgtgaacgatgtgctggcg ctgcgcaagcggattgcagcattgcgatggcgaaggcgatggcgcgaccgc cagattagcaacctggtgctgctggatagcgaatttaccaccctgccggatgtgctgtt gaaggccgcccgcgtggtgaacaacgtgtgcacttatccggcc
WP_021147403	aattgcagaattcatgtatagcgtggaaaccctggcgcgcgctggatgtgctgctg gataaaaccggcaccattaccagggcaaatgaccgtgaaaggcctgaaactg ctgagcgaacgctttaccaagaagaactggaacgcctgctggcggcgtatattgga acatagcaaaagataacaacgcgaccgcgaggcgattcgaacgcgctatgaagg cctggaacatcattatcaggtggcgatattattccgttagcagcgatcgcaaatgg ggcgcgatgagcattgatggcgtggcaccctgttctgggcgcgcggaaatgctg ctggaagaaaaccgaaagcgggtgatcaggcgcaggcgcgcggcagccgcgt gctgattctggcgtggagccagagcgcgggtggataccgaaacctagcctgccg aacgatgtggaaggcctggcgcgtgctggaatcgcgatccgattcgtgaagatgc ggcggaaaccctggaatatctgctagcgaagatgtaccctgaaaattattagcg gagataaccgggtgaccgtgagccatattgcgcatcaggcgggctttgaggattatc agagctatattgattgcagcaaatgagcgaatgaaactggaagcgtggcgga agataccgcgattttggccgctgagcccgcacagaaaaaactgctgattcagac cctgaacgcgaacggccataaccaccgcgatgaccggcgatggcgtgaacgatatt ctggcgcgtgcgcaagcggattgcagcattgtgatggcgaaggcgatccggcga cccggcagattgcgaacctggtgctgatggatagcgaatttaagatattccggaaa ttctgttgaaggccgcccgcgtggtgaacaacgtgtgcacttatccggcc
WP_053825032	aattgcagaattcatgaccaaccgggaacagcgcctgattgtgaccgatctggatg caccctgctgatgatgcgacgctttgaagaacgctttattaccagcgcagcatt gataccgtgaaacgcgatgatgctgggctatcgcttgcgggtggcgaccgcgcg cccggtagcaccggcttgaatatgcgggcaaacctgccgggtggatgctatattat ctgaacggcgcgctgattgatttgcgcccgaacgcagcgattatgatctgctgacca gcccggcctgcccagcgatggccatctgctgaaagtgggcttagcagcgcgcgcg gctgcaagtgctgcccgtatctgctggatgaaattccgggctgagcctggcattg tgatggatgatgtgcctataccaactttgatgtgagcgtgattgaaaaccagac ctggcagttaccgatttaccgatgtgccggatggcattgcggataaaattatttttc

	cgaaaagcgaacagtgggcgcatctgaaaaccctggtgccgccggatthgatg gcgattagcgaaggcagcatgtggatgctgatgagcccgctggcgaacaaacgcc aggcgctgaaaaccctgtgcaacgcatggatgtgacctggatggcaccgtgag ctttggcgatgatctgattgatattggcatgatgaccaccagcgaaccggcggtggcg gtggcgaacgcaaccgggaagtgataaaattgcggatgaaattgccgcca acaacgatgatggcggtggcgagtgattgaacgccatctgctggcggtgtcgact atccggcc
YP_003971091	aattgcagaattcatgcaacgtggtgctgctggatctggatggcaccctgacca gagcgatccgggcattattgctgctgcaacaaagcgtttgaagaactgagcctgc cgggtgccggatgatcaggaaatgcatcgctttattggcccggcattattgaaagcttt cgccgcaaccatgatccggatgaactgctggatcgcgcggtggaaattatcgca atattatgaggataaagcgggtgttgatgatccgaacaacccgggcccataaaattcc gggcccctgtataacagcgtgatgctggcattccggaacagctggcggcgctgc gctggatggcctgcatctggcgattgcaacctgcaaacccgagatcaggcgga accggtgtgcaacattttcatctggataccatggtggatggcatttatggcgagc accgataacagccgattgataaagatcaggtgattcgctattgctttgatagcattgg ctttgatgaggatgctggcgatcgcgctgatggtggcgatcgctggaccgatgt ggatggcgatgctgctggcctggattgctggcgctgcccgtgggctatgagg agcgggcaactggaagaacatggcgctatcgattattgataccgtggatgaac tggcgcgccgggtgaacgattattttgcaagttgtcgacttatccggcc
YP_003971333	aattgcagaattcatgataaagcggcgctttttgatattgatggcaccctgaccagcttt gtgaccatgtgattccgcagagcagcattgatgctgctgatgaactgcaggatcgc ggcgtgaaagtgtttatttgcagcggccgctgctgagccatgatccgtggtgctg gatgatgcccgtgcatthgatggcattattgctgctgaacggccagattgctttgatg atcatggcctgctgaaaaaagaaagcctgctgcccgaagatattgtgaccattacc gctggctggatgaacatccggatgtggtggcgaactattgcaaaaagattatgtga tttaaccagattaccgatgctgctgcaacctggcgccagctgggcaaacccg cgccgaccgtgaacattgatgatccgatgaacgcgctgaaacatgaaaccttt cagattagcccgtatattagctttgaagatgaagcgaactgagcggcatgtcccgc aacgtgctggcgctgctgctggatccggattttaccgatctgattccggcggtggc ggcaaacgggaaggatgaaacgctttatgctgattatggctggaccggcgaac agaccattgctttggcgatggcggaacgatgctggatgctggcgtttgaggga ttggcgtggcgatgggcaacgcgaccgaaccggcgaagcggcgccggtattat taccgatgatggatcatgatggcattatgaacgcgctgaaacattttacgtgctgg ttgtcgacttatccggcc

Supplemental Table 5: Gene fragments used to generate the standard curves for quantification of the 3EH genes by qPCR.

Bacterial EH Gene Fragments	
Gene	Sequence
NP_814872	ATGTCAATTAAGTTAGTTGCTATTGATATCGACGGAACAT TGCTAAATTCACAACACAAGATTACCCACGGGTCAAAGA AGCGCTCCAAAAGCAAATGAGCAAGGTGTTTCGTATTGTT TTATGTACAGGCCGTCTTT
YP_003971091	ACCGGCCATCATCGAGTCGTTTCAGACGCAACCATATGCC GGACGAGCTGCTGGACCGCGGCGTGGAGATATACCGCG AATACTATGCGGACAAGGCGGTGTTTCGACGACCCGAACA ATCCCGGCCACAAAATTCCCGGACGAC
YP_003971333	CCA ACTCGGCAAGACCGCACCGACCGTGAACATCGACG ATCCGCACGAGAGGGCGCTGAAGCATGAGACGTTCCAG ATCAGCCCGTACATCAGCTTTGAAGATGAAGCGAAGCTG TCC GGCATGTGTCGC

Supplemental Table 6: Estimated odds ratio based on univariate logistical regression models of atopy at age two or asthma at age four. Logistical regression was used to estimate the relationships between known early-life risk factors, log-transformed fecal 12,13 DiHOME concentration, or log-transformed 3EH copy number and the odds of developing atopy at age two or asthma at age four. Increased fecal 12,13 DiHOME was associated with significantly increased odds of atopy or asthma, while increased fecal 3EH copy number trended towards significance (shown in bold). These relationships did not exhibit strong evidence of confounding by the remaining early-life risk factors (change in odds ratios < 20%).

Univariate logistical regression models of atopy at age 2 and/or asthma at age 4		
	Odds Ratio (95% Confidence Interval)	P value
Race		
White	0.84 (0.16-4.36)	0.839
Black	0.62 (0.14-2.76)	0.532
Male	0.90 (0.26-3.07)	0.867
Age of Stool	0.99 (0.95-1.02)	0.517
Maternal Asthma	3.57 (0.60-21.1)	0.16
Cesarean Section	1.20 (0.26-5.63)	0.817
Exclusively Breastfed	0.35 (0.03-3.70)	0.384
Maternal Smoking	1.19 (0.21-6.72)	0.846
Environmental Smoke Exposure	2.47 (0.64-9.54)	0.189
No Pet Exposure	1.60 (0.42-6.11)	0.492
3EH	2.09 (0.93-4.68)	0.073
12,13 DiHOME	7.67(1.28-46.0)	0.026

Acknowledgements

We would like to acknowledge the WHEALS study participants, Dr. Anthony Iavarone and the mass spectrometry facility and genomic sequencing laboratory at QB3 Berkeley (<http://qb3.berkeley.edu/>), and generous plasmid donations by Drs. Oren Rosenberg, Bert Vogelstein, and Bruce Spiegelman. Nicolas Lukacs for critical assessment of the manuscript.

CHAPTER 3: Implications and Future Directions

In this study we aimed to establish a mechanism for how 12,13 DiHOME, a microbiome-associated metabolite identified in the stool of neonates at high-risk of atopy and asthma, modulates the immune system and to determine its source in the neonatal gut. *In vitro*, we found that 12,13 DiHOME acts via PPAR γ on DCs to decrease the frequency of Tregs. The effects of 12,13 DiHOME on CD36, a PPAR γ -regulated gene (Figure 1d), were consistent with those observed by others with 12,13 DiHOME treatment of adipose and skeletal muscle (Lynes et al., 2017; Stanford et al., 2018). While we were able to show that high concentrations of 12,13 DiHOME directly activate PPAR γ (Figure 1J), further studies are required to evaluate whether it is acting as a true activator or a competitive agonist at lower doses. Our *in vivo* data demonstrated that peritoneal delivery of 12,13 DiHOME exacerbates allergic airway inflammation in mice, while reducing the frequency of Tregs (Figure 2). Together these results indicate that increased fecal concentrations of 12,13 DiHOME in early-life may suppress immune tolerance, promoting allergic inflammation in the lungs during a critical window of immune and microbiological development.

Using metagenomic sequencing of neonatal fecal samples, we identified three functional bacterial genes, encoding enzymes capable of 12,13 DiHOME production *in vitro* (Figure 3d). Interestingly, of the three EH genes that could produce 12,13 DiHOME, two were found in strains of *Bifidobacterium bifidum*. *Bifidobacteria* are traditionally considered a marker of a healthy microbiome, and strains of *B. bifidum* are used as probiotics in humans (Hill et al., 2014; O'Callaghan and van Sinderen, 2016). In spite of this, we found that neonates with increased fecal abundance of specific *B. bifidum* and *E. faecalis* EH genes had increased odds of developing atopy and/or asthma in childhood (Figure 3e,f), indicating that strain-specific microbial functions may play a significant role in dictating microbial-immune interactions and clinical outcomes. Further studies are required to determine whether these specific enzymes and strains are sufficient to induce allergic airway inflammation in mice. However, our data emphasizes the need for strain level functional profiling of the microbiome and an understanding

of the end products of microbial gene expression that mediate important microbial-host interactions.

Fecal 12,13 DiHOME and the 3EH genes may serve as readouts of underlying early-life gut-microbiome dysbiosis resulting from convergent environmental exposures in early life; however, this hypothesis and the specific risk factors that lead to enrichment of strains with the capacity to produce high concentrations of this oxylipin require validation in multiple larger cohorts. Further studies are required to assess the contribution of microbial-derived 12,13 DiHOME in specific tissues and its dose-dependent effects on the immune system. In spite of these limitations, fecal 12,13 DiHOME and 3EH copy number offer an understanding of the microbial mechanisms of early-life immune dysfunction associated with disease development and the potential for early-life identification of neonates at risk of atopy and asthma years in advance of clinical symptoms.

REFERENCES

- Aichbaumik, N., Zoratti, E.M., Strickler, R., Wegienka, G., Ownby, D.R., Havstad, S., Johnson, C.C., 2008. Prenatal exposure to household pets influences fetal immunoglobulin E production. *Clin. Exp. Allergy* 38, 1787–1794. doi:10.1111/j.1365-2222.2008.03079.x
- Arrieta, M.-C., Stiemsma, L.T., Amenyogbe, N., Brown, E.M., Finlay, B., 2014. The Intestinal Microbiome in Early Life: Health and Disease. *Frontiers in Immunology* 5, 355. doi:10.3389/fimmu.2014.00427
- Arrieta, M.-C., Stiemsma, L.T., Dimitriu, P.A., Thorson, L., Russell, S., Yurist-Doutsch, S., Kuzeljevic, B., Gold, M.J., Britton, H.M., Lefebvre, D.L., Subbarao, P., Mandhane, P., Becker, A., McNagny, K.M., Sears, M.R., Kollmann, T., CHILD Study Investigators, Mohn, W.W., Turvey, S.E., Finlay, B.B., 2015. Early infancy microbial and metabolic alterations affect risk of childhood asthma. *Sci Transl Med* 7, 307ra152–307ra152. doi:10.1126/scitranslmed.aab2271
- Bahl, C.D., Morisseau, C., Bomberger, J.M., Stanton, B.A., Hammock, B.D., O'Toole, G.A., Madden, D.R., 2010. Crystal structure of the cystic fibrosis transmembrane conductance regulator inhibitory factor Cif reveals novel active-site features of an epoxide hydrolase virulence factor. *J. Bacteriol.* 192, 1785–1795. doi:10.1128/JB.01348-09
- Baker, K., Raemdonck, K., Dekkak, B., Snelgrove, R.J., Ford, J., Shala, F., Belvisi, M.G., Birrell, M.A., 2016. Role of the ion channel, transient receptor potential cation channel subfamily V member 1 (TRPV1), in allergic asthma. *Respiratory Research* 17, 143. doi:10.1186/s12931-016-0384-x
- Bao, Y., Chen, Z., Liu, E., Xiang, L., Zhao, D., Hong, J., 2017. Risk Factors in Preschool Children for Predicting Asthma During the Preschool Age and the Early School Age: a Systematic Review and Meta-Analysis. *Curr Allergy Asthma Rep* 17, 85. doi:10.1007/s11882-017-0753-7
- Bäckhed, F., Roswall, J., Peng, Y., Feng, Q., Jia, H., Kovatcheva-Datchary, P., Li, Y., Xia, Y., Xie, H., Zhong, H., Khan, M.T., Zhang, J., Li, J., Xiao, L., Al-Aama, J., Zhang, D., Lee, Y.S., Kotowska, D., Colding, C., Tremaroli, V., Yin, Y., Bergman, S., Xu, X., Madsen, L., Kristiansen, K., Dahlgren, J., Wang, J., 2015. Dynamics and Stabilization of the Human Gut Microbiome during the First Year of Life. *Cell Host Microbe* 17, 852. doi:10.1016/j.chom.2015.05.012
- Biswal, B.K., Morisseau, C., Garen, G., Cherney, M.M., Garen, C., Niu, C., Hammock, B.D., James, M.N.G., 2008. The molecular structure of epoxide hydrolase B from *Mycobacterium tuberculosis* and its complex with a urea-based inhibitor. *J. Mol. Biol.* 381, 897–912. doi:10.1016/j.jmb.2008.06.030
- Burke, H., Leonardi-Bee, J., Hashim, A., Pine-Abata, H., Chen, Y., Cook, D.G., Britton, J.R., McKeever, T.M., 2012. Prenatal and passive smoke exposure and incidence of asthma and wheeze: systematic review and meta-analysis. *Pediatrics* 129, 735–744. doi:10.1542/peds.2011-2196
- Byndloss, M.X., Olsan, E.E., Rivera-Chávez, F., Tiffany, C.R., Cevallos, S.A., Lokken, K.L., Torres, T.P., Byndloss, A.J., Faber, F., Gao, Y., Litvak, Y., Lopez, C.A., Xu, G., Napoli, E., Giulivi, C., Tsolis, R.M., Revzin, A., Lebrilla, C.B., Bäuml, A.J., 2017. Microbiota-activated PPAR- γ signaling inhibits dysbiotic Enterobacteriaceae expansion. *Science* 357, 570–575. doi:10.1126/science.aam9949
- Choo, J., Lee, Y., Yan, X.-J., Noh, T.H., Kim, S.J., Son, S., Pothoulakis, C., Moon, H.R., Jung, J.H., Im, E., 2015. A Novel Peroxisome Proliferator-activated Receptor (PPAR) γ Agonist 2-Hydroxyethyl 5-chloro-4,5-didehydrojasmonate Exerts Anti-Inflammatory Effects in Colitis. *J. Biol. Chem.* 290, 25609–25619. doi:10.1074/jbc.M115.673046

- Chu, S., Zhang, Y., Jiang, Y., Sun, W., Zhu, Q., Wang, B., Jiang, F., Zhang, J., 2017. Cesarean section without medical indication and risks of childhood allergic disorder, attenuated by breastfeeding. *Sci Rep* 7, 9762. doi:10.1038/s41598-017-10206-3
- DeAngelis, K.M., Brodie, E.L., DeSantis, T.Z., Andersen, G.L., Lindow, S.E., Firestone, M.K., 2009. Selective progressive response of soil microbial community to wild oat roots. *The ISME Journal* 3, 168–178. doi:10.1038/ismej.2008.103
- Decker, M., Arand, M., Cronin, A., 2009. Mammalian epoxide hydrolases in xenobiotic metabolism and signalling. *Arch. Toxicol.* 83, 297–318. doi:10.1007/s00204-009-0416-0
- Dominguez-Bello, M.G., Costello, E.K., Contreras, M., Magris, M., Hidalgo, G., Fierer, N., Knight, R., 2010. Delivery mode shapes the acquisition and structure of the initial microbiota across multiple body habitats in newborns. *Proc. Natl. Acad. Sci. U.S.A.* 107, 11971–11975. doi:10.1073/pnas.1002601107
- Donaldson, G.P., Lee, S.M., Mazmanian, S.K., 2016. Gut biogeography of the bacterial microbiota. *Nat. Rev. Microbiol.* 14, 20–32. doi:10.1038/nrmicro3552
- Durack, J., Kimes, N.E., Lin, D.L., Rauch, M., McKean, M., McCauley, K., Panzer, A.R., Mar, J.S., Cabana, M.D., Lynch, S.V., 2018. Delayed gut microbiota development in high-risk for asthma infants is temporarily modifiable by *Lactobacillus* supplementation. *Nat Commun* 9, 707. doi:10.1038/s41467-018-03157-4
- Fall, T., Lundholm, C., Örtqvist, A.K., Fall, K., Fang, F., Hedhammar, Å., Kämpe, O., Ingelsson, E., Almqvist, C., 2015. Early Exposure to Dogs and Farm Animals and the Risk of Childhood Asthma. *JAMA Pediatrics* 169, e153219–e153219. doi:10.1001/jamapediatrics.2015.3219
- Fischer, G.J., Keller, N.P., 2016. Production of cross-kingdom oxylipins by pathogenic fungi: An update on their role in development and pathogenicity. *J. Microbiol.* 54, 254–264. doi:10.1007/s12275-016-5620-z
- Fonseca, W., Lucey, K., Jang, S., Fujimura, K.E., Rasky, A., Ting, H.-A., Petersen, J., Johnson, C.C., Boushey, H.A., Zoratti, E., Ownby, D.R., Levine, A.M., Bobbit, K.R., Lynch, S.V., Lukacs, N.W., 2017. *Lactobacillus johnsonii* supplementation attenuates respiratory viral infection via metabolic reprogramming and immune cell modulation. *Mucosal Immunol* 10, 1569–1580. doi:10.1038/mi.2017.13
- Fujimura, K.E., Demoor, T., Rauch, M., Faruqi, A.A., Jang, S., Johnson, C.C., Boushey, H.A., Zoratti, E., Ownby, D., Lukacs, N.W., Lynch, S.V., 2014a. House dust exposure mediates gut microbiome *Lactobacillus* enrichment and airway immune defense against allergens and virus infection. *Proc. Natl. Acad. Sci. U.S.A.* 111, 805–810. doi:10.1073/pnas.1310750111
- Fujimura, K.E., Demoor, T., Rauch, M., Faruqi, A.A., Jang, S., Johnson, C.C., Boushey, H.A., Zoratti, E., Ownby, D., Lukacs, N.W., Lynch, S.V., 2014b. House dust exposure mediates gut microbiome *Lactobacillus* enrichment and airway immune defense against allergens and virus infection. *Proc. Natl. Acad. Sci. U.S.A.* 111, 805–810. doi:10.1073/pnas.1310750111
- Fujimura, K.E., Lynch, S.V., 2015. Microbiota in Allergy and Asthma and the Emerging Relationship with the Gut Microbiome. *Cell Host Microbe* 17, 592–602. doi:10.1016/j.chom.2015.04.007
- Fujimura, K.E., Sitarik, A.R., Havstad, S., Lin, D.L., Levan, S.R., Fadrosch, D., Panzer, A.R., LaMere, B., Rackaityte, E., Lukacs, N.W., Wegienka, G., Boushey, H.A., Ownby, D.R., Zoratti, E.M., Levin, A.M., Johnson, C.C., Lynch, S.V., 2016. Neonatal gut microbiota associates with childhood multisensitized atopy and T cell differentiation. *Nat. Med.* 22, 1187–1191. doi:10.1038/nm.4176
- Gallant, M.J., Ellis, A.K., 2018. What can we learn about predictors of atopy from birth cohorts and cord blood biomarkers? *Ann. Allergy Asthma Immunol.* 120, 138–144. doi:10.1016/j.anai.2017.12.003
- Genuneit, J., 2012. Exposure to farming environments in childhood and asthma and wheeze in rural populations: a systematic review with meta-analysis. *Pediatr Allergy Immunol* 23, 509–

518. doi:10.1111/j.1399-3038.2012.01312.x
- Gerlich, J., Benecke, N., Peters-Weist, A.S., Heinrich, S., Roller, D., Genuneit, J., Weinmayr, G., Windstetter, D., Dressel, H., Range, U., Nowak, D., Mutius, von, E., Radon, K., Vogelberg, C., 2017. Pregnancy and perinatal conditions and atopic disease prevalence in childhood and adulthood. *Allergy* 12, 39. doi:10.1111/all.13372
- Gilbert, J.A., Quinn, R.A., Debelius, J., Xu, Z.Z., Morton, J., Garg, N., Jansson, J.K., Dorrestein, P.C., Knight, R., 2016. Microbiome-wide association studies link dynamic microbial consortia to disease. *Nature* 535, 94–103. doi:10.1038/nature18850
- Gomez, G.A., Morisseau, C., Hammock, B.D., Christianson, D.W., 2006. Human soluble epoxide hydrolase: structural basis of inhibition by 4-(3-cyclohexylureido)-carboxylic acids. *Protein Sci.* 15, 58–64. doi:10.1110/ps.051720206
- Gonzalez-Perez, G., Hicks, A.L., Tekieli, T.M., Radens, C.M., Williams, B.L., Lamou  -Smith, E.S.N., 2016. Maternal Antibiotic Treatment Impacts Development of the Neonatal Intestinal Microbiome and Antiviral Immunity. *The Journal of Immunology* 196, 3768–3779. doi:10.4049/jimmunol.1502322
- Gouveia-Figueira, S., Karimpour, M., Bosson, J.A., Blomberg, A., Unosson, J., Pourazar, J., Sandstr  m, T., Behndig, A.F., Nording, M.L., 2017. Mass spectrometry profiling of oxylipins, endocannabinoids, and N-acyl ethanolamines in human lung lavage fluids reveals responsiveness of prostaglandin E2 and associated lipid metabolites to biodiesel exhaust exposure. *Anal Bioanal Chem* 409, 2967–2980. doi:10.1007/s00216-017-0243-8
- Gouveia-Figueira, S., Sp  th, J., Zivkovic, A.M., Nording, M.L., 2015. Profiling the Oxylipin and Endocannabinoid Metabolome by UPLC-ESI-MS/MS in Human Plasma to Monitor Postprandial Inflammation. *PLoS ONE* 10, e0132042. doi:10.1371/journal.pone.0132042
- Green, D., Ruparel, S., Gao, X., Ruparel, N., Patil, M., Akopian, A., Hargreaves, K., 2016. Central activation of TRPV1 and TRPA1 by novel endogenous agonists contributes to mechanical allodynia and thermal hyperalgesia after burn injury. *Mol Pain* 12, 174480691666172. doi:10.1177/1744806916661725
- Ha, J., Dobretsov, M., Kurten, R.C., Grant, D.F., Stimers, J.R., 2002. Effect of linoleic acid metabolites on Na(+)/K(+) pump current in N20.1 oligodendrocytes: role of membrane fluidity. *Toxicol. Appl. Pharmacol.* 182, 76–83.
- Hammad, H., de Heer, H.J., Soulli  , T., Angeli, V., Trottein, F., Hoogsteden, H.C., Lambrecht, B.N., 2004. Activation of peroxisome proliferator-activated receptor-gamma in dendritic cells inhibits the development of eosinophilic airway inflammation in a mouse model of asthma. *The American Journal of Pathology* 164, 263–271.
- Hartl, D., Koller, B., Mehlhorn, A.T., Reinhardt, D., Nicolai, T., Schendel, D.J., Griese, M., Krauss-Etschmann, S., 2007. Quantitative and functional impairment of pulmonary CD4+CD25hi regulatory T cells in pediatric asthma. *Journal of Allergy and Clinical Immunology* 119, 1258–1266. doi:10.1016/j.jaci.2007.02.023
- Havstad, S., Johnson, C.C., Kim, H., Levin, A.M., Zoratti, E.M., Joseph, C.L.M., Ownby, D.R., Wegienka, G., 2014. Atopic phenotypes identified with latent class analyses at age 2 years. *J. Allergy Clin. Immunol.* 134, 722–727.e2. doi:10.1016/j.jaci.2014.01.022
- Havstad, S., Wegienka, G., Zoratti, E.M., Lynch, S.V., Boushey, H.A., Nicholas, C., Ownby, D.R., Johnson, C.C., 2011. Effect of prenatal indoor pet exposure on the trajectory of total IgE levels in early childhood. *J. Allergy Clin. Immunol.* 128, 880–885.e4. doi:10.1016/j.jaci.2011.06.039
- Iyer, S.S., Cheng, G., 2012. Role of interleukin 10 transcriptional regulation in inflammation and autoimmune disease. *Crit. Rev. Immunol.* 32, 23–63.
- Kaminski, J., Gibson, M.K., Franzosa, E.A., Segata, N., Dantas, G., Huttenhower, C., 2015. High-Specificity Targeted Functional Profiling in Microbial Communities with ShortBRED. *PLoS Comput Biol* 11, e1004557. doi:10.1371/journal.pcbi.1004557
- Karonen, T., Neuvonen, P.J., Backman, J.T., 2012. CYP2C8 but not CYP3A4 is important in the

- pharmacokinetics of montelukast. *British Journal of Clinical Pharmacology* 73, 257–267. doi:10.1111/j.1365-2125.2011.04086.x
- Khare, A., Chakraborty, K., Raundhal, M., Ray, P., Ray, A., 2015. Cutting Edge: Dual Function of PPAR γ in CD11c⁺ Cells Ensures Immune Tolerance in the Airways. *J. Immunol.* 195, 431–435. doi:10.4049/jimmunol.1500474
- Knight, R., Callewaert, C., Marotz, C., Hyde, E.R., Debelius, J.W., McDonald, D., Sogin, M.L., 2017. The Microbiome and Human Biology. *Annu Rev Genomics Hum Genet* 18, 65–86. doi:10.1146/annurev-genom-083115-022438
- Langdon, A., Crook, N., Dantas, G., 2016. The effects of antibiotics on the microbiome throughout development and alternative approaches for therapeutic modulation. *Genome Med* 8, 39. doi:10.1186/s13073-016-0294-z
- Lecka-Czernik, B., Moerman, E.J., Grant, D.F., Lehmann, J.M., Manolagas, S.C., Jilka, R.L., 2002. Divergent effects of selective peroxisome proliferator-activated receptor-gamma 2 ligands on adipocyte versus osteoblast differentiation. *Endocrinology* 143, 2376–2384. doi:10.1210/endo.143.6.8834
- Lodge, C.J., Allen, K.J., Lowe, A.J., Hill, D.J., Hosking, C.S., Abramson, M.J., Dharmage, S.C., 2012. Perinatal cat and dog exposure and the risk of asthma and allergy in the urban environment: a systematic review of longitudinal studies. *Clinical and Developmental Immunology* 2012, 176484–10. doi:10.1155/2012/176484
- Lundström, S.L., Levänen, B., Nording, M., Klepczynska-Nyström, A., Sköld, M., Haeggström, J.Z., Grunewald, J., Svartengren, M., Hammock, B.D., Larsson, B.-M., Eklund, A., Wheelock, Å.M., Wheelock, C.E., 2011. Asthmatics exhibit altered oxylipin profiles compared to healthy individuals after subway air exposure. *PLoS ONE* 6, e23864. doi:10.1371/journal.pone.0023864
- Lundström, S.L., Yang, J., Källberg, H.J., Thunberg, S., Gafvelin, G., Haeggström, J.Z., Grönneberg, R., Grunewald, J., van Hage, M., Hammock, B.D., Eklund, A., Wheelock, Å.M., Wheelock, C.E., 2012. Allergic asthmatics show divergent lipid mediator profiles from healthy controls both at baseline and following birch pollen provocation. *PLoS ONE* 7, e33780. doi:10.1371/journal.pone.0033780
- Lynch, S.V., Pedersen, O., 2016. The Human Intestinal Microbiome in Health and Disease. *N. Engl. J. Med.* 375, 2369–2379. doi:10.1056/NEJMra1600266
- Lynes, M.D., Leiria, L.O., Lundh, M., Bartelt, A., Shamsi, F., Huang, T.L., Takahashi, H., Hirshman, M.F., Schlein, C., Lee, A., Baer, L.A., May, F.J., Gao, F., Narain, N.R., Chen, E.Y., Kiebish, M.A., Cypess, A.M., Blüher, M., Goodyear, L.J., Hotamisligil, G.S., Stanford, K.I., Tseng, Y.-H., 2017. The cold-induced lipokine 12,13-diHOME promotes fatty acid transport into brown adipose tissue. *Nat. Med.* 37, 1685. doi:10.1038/nm.4297
- Mitre, E., Susi, A., Kropp, L.E., Schwartz, D.J., Gorman, G.H., Nylund, C.M., 2018. Association Between Use of Acid-Suppressive Medications and Antibiotics During Infancy and Allergic Diseases in Early Childhood. *JAMA Pediatrics* e180315. doi:10.1001/jamapediatrics.2018.0315
- Morisseau, C., 2013. Role of epoxide hydrolases in lipid metabolism. *Biochimie* 95, 91–95. doi:10.1016/j.biochi.2012.06.011
- Mosblech, A., Feussner, I., Heilmann, I., 2009. Oxylipins: structurally diverse metabolites from fatty acid oxidation. *Plant Physiol. Biochem.* 47, 511–517. doi:10.1016/j.plaphy.2008.12.011
- Nobs, S.P., Natali, S., Pohlmeier, L., Okreglicka, K., Schneider, C., Kurrer, M., Sallusto, F., Kopf, M., 2017. PPAR γ in dendritic cells and T cells drives pathogenic type-2 effector responses in lung inflammation. *J Exp Med* 8, jem.20162069. doi:10.1084/jem.20162069
- Ober, C., Yao, T.-C., 2011. The genetics of asthma and allergic disease: a 21st century perspective. *Immunol. Rev.* 242, 10–30. doi:10.1111/j.1600-065X.2011.01029.x
- Silvers, K.M., Frampton, C.M., Wickens, K., Pattermore, P.K., Ingham, T., Fishwick, D., Crane, J., Town, G.I., Epton, M.J., New Zealand Asthma and Allergy Cohort Study Group, 2012.

- Breastfeeding protects against current asthma up to 6 years of age. *J. Pediatr.* 160, 991–6.e1. doi:10.1016/j.jpeds.2011.11.055
- Simpson, A., Tan, V.Y.F., Winn, J., Svensén, M., Bishop, C.M., Heckerman, D.E., Buchan, I., Custovic, A., 2010. Beyond atopy: multiple patterns of sensitization in relation to asthma in a birth cohort study. 181, 1200–1206. doi:10.1164/rccm.200907-1101OC
- Sminkey, L. (Ed.), n.d. Chronic respiratory diseases [WWW Document]. World Health Organization. URL <http://www.who.int/respiratory/asthma/en/> (accessed 5.10.18).
- Smit, M.S., 2004. Fungal epoxide hydrolases: new landmarks in sequence-activity space. *Trends Biotechnol.* 22, 123–129. doi:10.1016/j.tibtech.2004.01.012
- Stanford, K.I., Lynes, M.D., Takahashi, H., Baer, L.A., Arts, P.J., May, F.J., Lehnig, A.C., Middelbeek, R.J.W., Richard, J.J., So, K., Chen, E.Y., Gao, F., Narain, N.R., Distefano, G., Shettigar, V.K., Hirshman, M.F., Ziolo, M.T., Kiebish, M.A., Tseng, Y.-H., Coen, P.M., Goodyear, L.J., 2018. 12,13-diHOME: An Exercise-Induced Lipokine that Increases Skeletal Muscle Fatty Acid Uptake. *Cell Metab.* 27, 1111–1120.e3. doi:10.1016/j.cmet.2018.03.020
- Suzek, B.E., Wang, Y., Huang, H., McGarvey, P.B., Wu, C.H., UniProt Consortium, 2015. UniRef clusters: a comprehensive and scalable alternative for improving sequence similarity searches. *Bioinformatics* 31, 926–932. doi:10.1093/bioinformatics/btu739
- Szatmari, I., Torocsik, D., Agostini, M., Nagy, T., Gurnell, M., Barta, E., Chatterjee, K., NAGY, L., 2007a. PPAR regulates the function of human dendritic cells primarily by altering lipid metabolism. *Blood* 110, 3271–3280. doi:10.1182/blood-2007-06-096222
- Szatmari, I., Torocsik, D., Agostini, M., Nagy, T., Gurnell, M., Barta, E., Chatterjee, K., NAGY, L., 2007b. PPAR regulates the function of human dendritic cells primarily by altering lipid metabolism. *Blood* 110, 3271–3280. doi:10.1182/blood-2007-06-096222
- Tang, L., Liu, Y., Jiang, R., Zheng, Y., Zheng, K., Zheng, H., 2015. A high-throughput adrenaline test for the exploration of the catalytic potential of halohydrin dehalogenases in epoxide ring-opening reactions. *Biotechnology and Applied Biochemistry* 62, 451–457. doi:10.1002/bab.1278
- Thompson, D.A., Hammock, B.D., 2007. Dihydroxyoctadecamonoenoate esters inhibit the neutrophil respiratory burst. *J. Biosci.* 32, 279–291.
- Trompette, A., Gollwitzer, E.S., Yadava, K., Sichelstiel, A.K., Sprenger, N., Ngom-Bru, C., Blanchard, C., Junt, T., Nicod, L.P., Harris, N.L., Marsland, B.J., 2014. Gut microbiota metabolism of dietary fiber influences allergic airway disease and hematopoiesis. *Nat. Med.* 20, 159–166. doi:10.1038/nm.3444
- Vangaveti, V.N., Shashidhar, V.M., Rush, C., Malabu, U.H., Rasalam, R.R., Collier, F., Baune, B.T., Kennedy, R.L., 2014. Hydroxyoctadecadienoic Acids Regulate Apoptosis in Human THP-1 Cells in a PPAR γ -Dependent Manner. *Lipids* 49, 1181–1192. doi:10.1007/s11745-014-3954-z
- Wahli, W., Michalik, L., 2012. PPARs at the crossroads of lipid signaling and inflammation. *Trends in Endocrinology & Metabolism* 23, 351–363. doi:10.1016/j.tem.2012.05.001
- Wang, Q., Bai, X., Xu, D., Xu, D., Li, H., Fang, J., Zhu, H., Fu, W., Cai, X., Wang, J., Jin, Z., Wang, Q., Xu, C., Chang, J., 2009. [TRPV1 UTR-3 polymorphism and susceptibility of childhood asthma of the Han Nationality in Beijing]. *Wei Sheng Yan Jiu* 38, 516–521.
- Wegienka, G., Havstad, S., Kim, H., Zoratti, E., Ownby, D., Woodcroft, K.J., Johnson, C.C., 2017. Subgroup differences in the associations between dog exposure during the first year of life and early life allergic outcomes. *Clin. Exp. Allergy* 47, 97–105. doi:10.1111/cea.12804
- Wegienka, G., Havstad, S., Zoratti, E.M., Kim, H., Ownby, D.R., Johnson, C.C., 2015. Combined effects of prenatal medication use and delivery type are associated with eczema at age 2 years. *Clin. Exp. Allergy* 45, 660–668. doi:10.1111/cea.12467
- Woerly, G., Honda, K., Loyens, M., Papin, J.-P., Auwerx, J., Staels, B., Capron, M., Dombrowicz, D., 2003. Peroxisome proliferator-activated receptors alpha and gamma down-regulate allergic inflammation and eosinophil activation. *J Exp Med* 198, 411–421.

doi:10.1084/jem.20021384


Yamamoto-Hanada, K., Yang, L., Narita, M., Saito, H., Ohya, Y., 2017. Influence of antibiotic use in early childhood on asthma and allergic diseases at age 5. *Ann. Allergy Asthma Immunol.* 119, 54–58. doi:10.1016/j.anai.2017.05.013

Ye, F., Zhang, Z.-S., Luo, H.-B., Shen, J.-H., Chen, K.-X., Shen, X., Jiang, H.-L., 2005. The Dipeptide H-Trp-Glu-OH Shows Highly Antagonistic Activity against PPAR γ : Bioassay with Molecular Modeling Simulation. *ChemBioChem* 7, 74–82. doi:10.1002/cbic.200500186

Publishing Agreement

It is the policy of the University to encourage the distribution of all theses, dissertations, and manuscripts. Copies of all UCSF theses, dissertations, and manuscripts will be routed to the library via the Graduate Division. The library will make all theses, dissertations, and manuscripts accessible to the public and will preserve these to the best of their abilities, in perpetuity.

I hereby grant permission to the Graduate Division of the University of California, San Francisco to release copies of my thesis, dissertation, or manuscript to the Campus Library to provide access and preservation, in whole or in part, in perpetuity.

Author Signature  Date 05/23/2018